COLORADO
Department of Transportation

CDOT Applied Research and Innovation Branch

An Investigation into Expansion Joint Movement for Integral Abutment Concrete Bridges

Rebecca Atadero, Aaron Wood

12/31/2023

Report No. 2024-02

The contents of this report reflect the views of the author(s), who is(are) responsible for the facts and accuracy of the data presented herein. The contents do not necessarily reflect the official views of the Colorado Department of Transportation or the Federal Highway Administration. This report does not constitute a standard, specification, or regulation.

Technical Report Documentation Page

1. Report No.	2. Government Accession No.	3. Recipient's Catalog No.
CDOT-2024-02		

4. Title and Subtitle	5. Report Date
An Investigation into Expansion Joint Movement for Integral Abutment Concrete Bridges	December 2023
	6. Performing Organization Code

7. Author(s)	8. Performing Organization Report No.
Aaron Wood, Rebecca Atadero	

9. Performing Organization Name and Address	10. Work Unit No. (TRAIS)
Colorado State University 711 Oval Drive Fort Collins, CO 80521	11. Contract or Grant No. 222-02

12. Sponsoring Agency Name and Address	13. Type of Report and Period Covered
Colorado Department of Transportation - Applied Research and Innovation Branch 2829 Howard Pl. Denver CO, 80204	Final
	14. Sponsoring Agency Code

15. Supplementary Notes

Prepared in cooperation with the US Department of Transportation, Federal Highway Administration

16. Abstract

Expansion joints on bridge structures allow for essential thermal movements of structural components but often at the cost of regular maintenance and periodic replacement to counter damage the joint may experience throughout its lifecycle. This project was conducted to study the potential for eliminating or removing expansion joints for one of the Colorado Department of Transportation's most common design types for new bridges: integral abutment, concrete bulb-T girder bridges. Eight bridges were selected for study. Joint movements over the course of a year were observed using scratch gauges and potentiometers. The measured joint movements were compared to the theoretical thermal movement calculated using industry standard design equations presented in AASHTO. AASHTO has two methods to estimate thermal movement, Procedure A and Procedure B. Procedure B was found to produce more accurate estimates of bridge movement, yet almost always overpredicted movement. The difference between the observed and theoretical movement for the single-span structures analyzed in this study was found to range from 0.347 to 0.051 inches, while the difference for multi-span structures was found to range from 0.830 to 0.439 inches. Additionally, comparisons between local weather station data and temperature contour maps presented in AASHTO Procedure B show high correlation. Based on the findings of this study, AASHTO Procedure B should be used to determine the theoretical thermal movement of a joint as CDOT recommends. Additionally, further investigation of longer, multi-span integral abutment bridges is needed to determine if a reduction coefficient for predicted movement may be appropriate.

17. Keywords	18. Distribution Statement
Expansion joints, Thermal movement, Integral abutment bridges	This document is available on CDOT's website https://www.codot.gov/programs/research

19. Security Classif. (of this report)	20. Security Classif. (of this page)	21. No. of Pages	22. Price
Unclassified	Unclassified		

Form DOT F 1700.7 (8-72) Reproduction of completed page authorized

Acknowledgements

The authors gratefully acknowledge the support of the CDOT study panel members, including Samuel Abraham, Brendan McGuire, Stephanie Rasmussen, and Jessica Martinez, who helped identify the bridges for study and answered many questions about bridge expansion joints during this project.

Table of Contents

Abstract

Expansion joints on bridge structures allow for essential thermal movements of structural components but often at the cost of regular maintenance and periodic replacement to counter damage the joint may experience throughout its lifecycle. This project was conducted to study the potential for eliminating or removing expansion joints for one of the Colorado Department of Transportation's most common design types for new bridges: integral abutment, concrete bulb-T girder bridges. Eight bridges were selected for study. Joint movements over the course of a year were observed using scratch gauges and potentiometers. The measured joint movements were compared to the theoretical thermal movement calculated using industry standard design equations presented in AASHTO. AASHTO has two methods to estimate thermal movement, Procedure A and Procedure B. Procedure B was found to produce more accurate estimates of bridge movement, yet almost always overpredicted movement. The difference between the observed and theoretical movement for the single-span structures analyzed in this study was found to range from 0.347 to 0.051 inches, while the difference for multi-span structures was found to range from 0.830 to 0.439 inches. Additionally, comparisons between local weather station data and temperature contour maps presented in AASHTO Procedure B show high correlation. Based on the findings of this study, AASHTO Procedure B should be used to determine the theoretical thermal movement of a joint as CDOT recommends. Additionally, further investigation of longer, multi-span integral abutment bridges is needed to determine if a reduction coefficient for predicted movement may be appropriate.

Executive Summary

Expansion joints allow bridges to undergo movement due to changes in temperature, thereby preventing damage that can be caused by restrained motion. However, expansion joints, particularly those of the strip seal type, are also a maintenance headache as they are prone to damage from snowplows, clogging, and deicing agents. Many new CDOT bridges are designed with integral abutments, and CDOT engineers suspect that bridges of this type may not experience as much expansion joint movement as predicted by the AASHTO code because thermal movements are either restrained or accommodated by other parts of the bridge assembly. This study measures expansion joint movements on actual bridges over the course of one year and compares these displacements to the movement predicted by bridge design codes.

Integral abutment bridges are the preferred bridge design for many state departments of transportation, including CDOT, because they eliminate bridge joints and the associated maintenance the joints require. CDOT commonly uses a design where the bridge superstructure and approach slab are both integrally connected at the abutment, and a joint is placed at the far end of the approach slab. Strip seal joints are used at this joint as they can accommodate movements up to four inches, but even at this location the joints are subject to damage and require a lot of maintenance. AASHTO provides two different methods for prediction of changes in bridge length due to changes in temperature, Procedure A and Procedure B. Both methods for predicting bridge movement were compared to field measurements.

Eight bridges were chosen for instrumentation based on a set of selection criteria intended to provide consistent conditions for joint movement measurements. Six bridges were concrete bulb tee girder bridges and two bridges were concrete box girder bridges. Bridges were located primarily along the Northern Front Range to provide for convenient access to Colorado State University. Scratch gauges were selected as simple but effective devices for measuring joint movement. A prototype gauge design was tested in the laboratory before installation on the bridges. In addition to the scratch gauges, electrical instrumentation including potentiometers for measuring displacement and temperature gauges were installed on two bridges to verify scratch gauge measurements.

The AASHTO LRFD Bridge Design Code includes two Procedures, A and B, to compute the theoretical thermal expansion of bridge elements, and thus movement of bridge joints. Both procedures were used to predict the movement of the expansion joints on the study bridges. Procedure A consistently predicts a smaller amount of movement than Procedure B, because Procedure A relies on a smaller, fixed, temperature range in the calculations. For some study bridges, the predicted movement was small enough that a small movement joint, rather than a strip seal joint, may have been appropriate.

After the scratch and displacement gauges had been installed on the bridges for about fifteen months, joint displacement measurements were collected. The temperature sensors and local weather data showed close correlation to the temperatures recommended in AASHTO Procedure B. Scratch gauge measurements compared well with the potentiometer measurements on the one bridge where the DAQ was still working at the time of data collection. Comparing the scratch gauge measurements to the theoretical movements computed following AASHTO showed that Procedure A consistently underpredicted joint movement, which could lead to undersized joints. Procedure B generally slightly overpredicted joint movement for single span bridges. For two-span bridges, Procedure B overpredicted the movement, and the actual movement was less than 60% of theoretical movement.

This study found that for single span concrete blub tee and concrete box girders, the AASHTO Procedure B method for predicting expansion joint movement is appropriate for design. AASHTO Procedure B seems to be too conservative for multi-span concrete bulb tee and concrete box girder bridges. The

findings of this study are limited by the small number of bridges analyzed. Joint movements on multi-span bridges especially warrant further study.

List of Figures

List of Tables

List of Abbreviations

AASHTO = American Association of State Highway and Transportation Officials

BDM = Bridge Design Manual

CBT = Concrete Bulb Tee

CDOT = Colorado Department of Transportation

DAQ = Data Acquisition System

IAB = Integral Abutment Bridges

LRFD = Load and Resistance Factor Design

NOAA = National Oceanic and Atmospheric Association

SIAB = Semi-integral Abutment Bridge

UTM = Universal Testing Machine

Chapter 1 Introduction

Problem Statement

The Colorado Department of Transportation's (CDOT's) typical structure for bridge replacements is precast Concrete Bulb Tee (CBT) girders supported on integral abutments with expansion joints at the end of the approach slabs. A typical section of a CDOT CBT girder is shown in Figure 1-1.

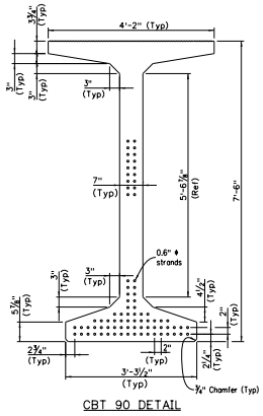

Figure 1-1 Typical section of a CDOT CBT girder (CDOT Standard Details)

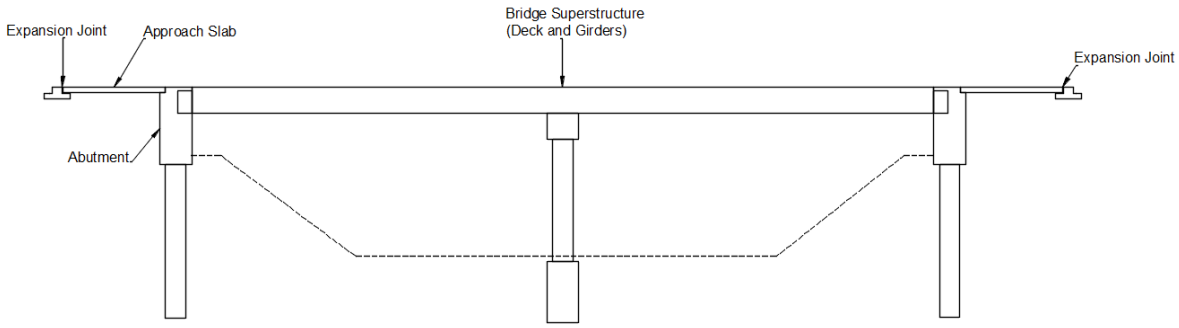

Figure 1-2 Bridge schematic showing expansion joint location

Based on experience regarding durability, maintenance, life-cycle costs, etc., the CDOT Bridge Design Manual (2023) lists recommended bridge joints in Section 14.4. The recommended joints are classified into small movement joints (movements up to ¾"), strip seals (movements up to 4") and modular joints (movements more than 4"). Based on common bridge lengths in Colorado, estimated joint movements calculated for most bridges following the AASHTO LRFD Bridge Design Code (2020) are in the range of 1 to 3 inches at the end of each approach slab. Thus, most new bridges are equipped with two 0-4" strip seal joints, one at the end of each approach slab.

A strip seal joint is one of multiple commonly used expansion joints consisting of metal rails on each side of the joint opening, connected via a neoprene gland which spans the joint opening as shown in Figure 1-3. Neoprene is a synthetic rubber that is less sensitive to temperature changes than natural rubber, which can become brittle in cold weather and sticky in hot weather (American Chemistry Council, 2022).

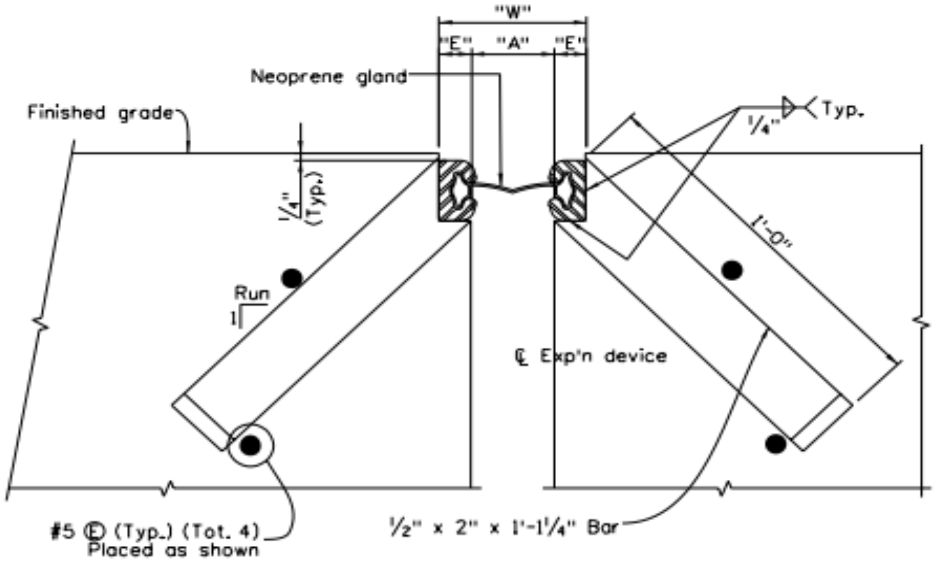

Figure 1-3 Cross-section of strip-seal expansion joint (from CDOT Bridge Design Manual Example Calculations)

Neoprene's durable yet flexible properties and its lack of response to temperature variation makes for a desirable solution to span bridge joint openings to prevent clogging and structurally damaging surface leaks. Although proven effective, normal wear and tear can cause structural deficiencies around and below the joint.

Although they are the CDOT recommended joint type, strip seal joints pose a variety of maintenance challenges. Causes of damage and deterioration include the operation and use of snowplows and chains during winter months as they hit the steel rails in strip seal joints causing physical damage; deicing salts penetrating the joint leading to corrosion of structural elements; and clogging from debris and vegetation which leads to acute stress build up resulting in spalling of the concrete deck. Damaged expansion joints reduce civilian comfort and when in residential areas, noise effects caused by uneven pavement must be carefully considered (Davidson, White, and Khan, 2012). Pursuant to manufacturer recommendations, strip seals should last between 15 and 20 years and should be replaced in their entirety rather than in phases. Strip seal joint replacements involve replacement of the surrounding concrete headers, also referred to as sleeper slabs, and the total replacement time is about four days. In many cases, bridges cannot be closed to service that long; therefore, strip seals have been replaced in phases with a weld joint in the middle. This practice reduces the life of the replacement joint. The damage becomes a safety hazard and joints are difficult for CDOT maintenance personnel to repair.

While strip seal joints are causing maintenance problems for CDOT, the necessity of these joints on integral abutment bridges is also questioned. Bridge movements for integral abutment bridges (IABs) are believed to be less than predicted by the bridge design code due to the unaccounted-for lateral deflection absorbed by abutment piles, soil-spring behavior of backfill and subgrade, and an overestimation of thermal effects on precast, prestressed superstructures (CDOT Bridge Design Manual 2023).

The purpose of this study is to measure actual bridge movements and, if bridge movements are indeed smaller than predicted by the design code, to derive a reduction coefficient for the expansion joint movement calculation for CBT girder bridges on integral abutments. With reduced predicted joint movements, it may become possible to eliminate strip seal joints and their associated maintenance, or investigate other joint options with less frequent maintenance requirements.

Scope and Objectives of Research

This research study included the following tasks:

- Identifying CBT girder bridges with integral abutments across Colorado.
- Identifying appropriate sensors to collect and store data about bridge movements and air temperature.
- Measuring bridge joint movement throughout the year using both electrical and mechanical sensors.
- Comparing recorded bridge movements to those calculated by the AASHTO design equation.
- Determining if a reduction coefficient should be implemented in expansion joint movement calculations for CBT girder bridges on integral abutments or suggesting other design accommodations.

Through this work, the hope is to reduce the number of new bridges with strip seal joints and, therefore, minimize the costs of joints and joint replacement; increase safety by avoiding steel rails on the roadway surface; and reduce time and effort spent by CDOT regional and maintenance personnel in replacing or repairing the joints.

Report Organization

To establish the context for this study, Chapter 2 of this report provides background information including a general understanding of integral abutment bridges; introductory information about expansion joints; and current AASHTO provisions used to predict bridge joint movement.

Bridge selection criteria (geographic regions, characteristics, accessibility, etc.) and the study bridges as well as gauge selection and implementation are described in Chapter 3. Chapter 4 discusses theoretical movements of the selected bridges in accordance with current CDOT design practices based on the LRFD code. Chapter 5 presents results from the displacement and temperature gauges installed on the bridges. These data are directly compared to the theoretical joint movement values presented in Chapter 4, and conclusions are drawn about the accuracy of bridge joint movement predictions following AASHTO guidance. Chapter 6 provides a brief summary of the study and conclusions and areas for further research.

Background

Integral Abutment Bridges

Integral abutment bridges first came into use in the 1960s as the maintenance issues associated with bridge expansion joints became clear and bridge owners sought to eliminate expansion joints (Arsoy, Barker and Duncan 1999). Integral abutments can be constructed in a variety of ways, including frame

abutments, embedded abutments, bank pad abutments, and end screen abutments (Lui, Han and Parsons 2022). In all cases the bridge superstructure elements such as girders are rigidly connected to the abutment or pier. Integral abutments are preferred by the CDOT Bridge Design Manual (BDM) (2023):

> "Integral abutments are preferred for most bridges due to the elimination of expansion joints (on the bridge deck) and bearings at supports, simplified construction, and reduced maintenance costs. Integral abutments rigidly attach both superstructure and supporting foundation elements so that the thermal translation and girder end rotations are transferred from the superstructure through the abutment to the foundation elements. The superstructure and substructure act as a single structural unit by distributing system flexibilities throughout the soil."

The performance of integral abutment bridges has attracted significant research attention from many state DOTs (for example, Virginia (Arsoy, Barker and Duncan 1999), Illinois (LaFave, 2017) and Indiana (Frosch and Lovell, 2011)). Although fully integral bridges do not have expansion joints to allow for movement of the bridge superstructure, changes in temperature still cause bridge elements to expand and contract and thus movements must be accommodated in other portions of the bridge system, or significant thermal stresses may be generated within the superstructure. Often movement is accommodated through rotation of abutments, piers, or foundations and the geotechnical design of abutments and supporting piles is significant to integral abutment bridge designs (Lui, Han and Parsons 2022).

The CDOT BDM acknowledges the need for movement in the piles as the preferred pile orientation is to align the weak axis of the pile with the centerline of the abutment to promote weak axis bending to tolerate longitudinal movement. Weak axis bending generates less resisting force in the piles from unintended frame-action with the superstructure and better accommodates bridge displacements, when compared with strong axis bending (CDOT 2023).

Although considered an integral abutment, often CDOT bridge designs include an expansion joint at the end of the approach slab (away from the bridge abutment) where undesired structural damage is not as critical, as shown in Figure 1-2. This detail was investigated by Phares et.al (2013) as a method to reduce the "bump at the end of the bridge" caused by settlement and cracking of the approach slab when the approach slab is not integrated with the abutment. In this type of bridge construction, as the bridge superstructure expands in warm temperatures, the abutment will push against the approach slab and friction between the slab and the ground may resist some of the movement. The expansion joint at the end of the approach slab is expected to accommodate movement from the bridge expansion and approach slab expansion (Phares et.al. 2013).

Disadvantages to fully integral abutment bridges include restrictions on the maximum length of bridge allowed to be designed as such. CDOT limits the design length for concrete structures to 460 feet (CDOT BDM Table 11-1) with the goal of limiting movement in one direction (either expanding or contracting) to 2 inches. Although longer unit span lengths have been achieved, detailed modeling must be done to prove the maximum movement at the expansion joint can be accommodated by a commonly used joint.

Bridge Expansion Joints

Expansion joints are used to create a smooth riding surface on the bridge deck for drivers and allow for thermal expansion and contraction of bridge structures while protecting structural components below from deicing salts and other harmful foreign objects. Joints can vary significantly in size, material, and

purpose based on structure type and length, expected climate exposure, and DOT preference (Chang and Lee 2002).

Expansion joints can be classified into two overarching categories: small movement joints and large movement joints. Within each category, a variety of materials can be used to accomplish the common goal of allowing for thermal movement while maintaining structural integrity and safety of the structure.

Small movement joints are typically used when the structure is expected to experience a thermal movement range of less than two inches. Small movement joints feature adhesive or steel edge rails mounted within the concrete to provide a watertight seal. Common types of small movement joints include asphalt fill, pourable silicone seals, and neoprene strip seal expansion joints. Neoprene strip seal joints can accommodate movements up to four inches while allowing for the neoprene to be replaced as required over the structure's service life, making strip seal joints a favorable option for a wide range of structures. Asphaltic plug joints are not favored by some DOTs as they may not expand and contract as much as anticipated. The purpose of selecting silicone and neoprene as expansive materials is due to their durable yet flexible properties which allow them to withstand repetitive tire contact and adverse climate conditions while allowing for thermal movements.

When a bridge joint is expected to experience larger movements, typically greater than four inches, large movement joints are utilized. Large expansion joints are designed to span a larger opening and support the weight of vehicles passing over the joint while allowing for thermal movements. Common large movement joints include finger joints, plate joints, and modular joints. Finger joints are comprised of teeth-like steel plates mounted on both sides of the joint which can then open or close while providing ample coverage of the joint to support traffic and prevent large debris from clogging the joint below. Similar to other joint types, issues may arise when using finger joints when the metal or neoprene trough below the joint may become clogged. This can be more common in finger joints as water can penetrate the openings between the fingers, carrying foreign objects to the trough below. Modular joints are similar to strip seal joints in that they utilize neoprene strips and steel beams as the attachment to the structure, but modular joints feature multiple neoprene strips and steel beams in order to span joints four inches or larger.

Regardless of the joint installed on a bridge, rideability and structural integrity are of utmost importance. Damaged or uneven joints can provide an uneven riding service, which poses safety risks to all vehicles, especially motorcyclists. Additionally, when vehicles pass over uneven joints, noise pollution from the contact between the tires and the joint can become a concern, especially in urban areas. Uneven joints are caused by uneven structure settlement, joint degradation or absence of a joint, and damage from clogging or snowplows. Clogging is the most common form of joint degradation, which can limit bridge movement resulting in additional stresses at joint locations and ultimately cracked or spalling of decks or roadway surfaces. Cracks within the surface of the bridge pose a risk to the structure below as water and deicing agents can penetrate the concrete and cause adverse effects to the structural components of the bridge. Maintenance of expansion joints is a costly endeavor as access to the joint may be difficult depending on bridge geometry and location. Full joint replacement requires a multi-day travel way closure while joint cleaning can be completed in less than a day if the joint is easily accessible. Regular joint cleaning, commonly done by using a power washer, vacuum truck, or sweeping and shoveling (Caltrans 2019), is believed to increase a joint's service life but it is not apparent whether the cost of such preventative programs outweigh the life cycle cost of replacing the joints (Bergdorfer, Berman, and Roeder 2013).

Thermal Effects on Bridges

There have been many detailed studies of bridge behavior due to thermal effects, including both computational analyses and field measurements. Many more recent studies tend to emphasize the thermal

effects on complex structures such as cable-stayed, suspension and arch bridges. Studies that do consider beam bridges have often focused on bridges with curves, skew, or other characteristics that make the thermal behavior more complex (Li et.al. 2023). Detailed analyses of thermal effects are often conducted as part of structural health monitoring as thermal effects can be larger than and obscure movements due to applied loads (Li et.al 2023).

The current research project was conducted to gain a preliminary understanding of a much simpler question: Are the predictions of bridge movement from the AASHTO LRFD Bridge Design Code appropriate for sizing of expansion joints at the end of approach slabs for bridges with integral abutments. For this reason, the background on thermal movement focuses on the current design procedures.

Current CDOT and AASHTO Provisions for Thermal Movement

Within Section 14 of the CDOT BDM, titled "Joints and Bearings", Section 14.2 states "Unless otherwise noted, the design of joints and bearings shall be in accordance with the latest AASHTO". This is followed by Section 14.3, titled "Uniform Temperature Movement", which states "Temperature ranges for either Procedure A or B (preferred) may be used for structures designed in accordance with AASHTO 3.12.2, along with the appropriate load factors provided in AASHTO Table 3.4.1-1. Temperature gradient may be considered where appropriate in accordance with AASHTO 3.12.3."

As mentioned in the CDOT BDM, the governing section of AASHTO for determining thermal movements of structures is 3.12 Force Effects Due to Superimposed Deformations. AASHTO 3.12.2 begins with "Either Procedure A or Procedure B may be employed for concrete deck bridges having concrete or steel girders." The section describes two methods alluded to in the CDOT BDM which are permitted to be used: Procedure A found in section 3.12.2.1 and Procedure B found in section 3.12.2.2, discussed further in the following sections. These sections of AASHTO define procedures used to determine the temperature range required to calculate the design thermal movement range, Δ_T, as defined in AASHTO 3.12.2.3:

$$\Delta_T = \alpha L(T_{MaxDesign} - T_{MinDesign}) \qquad \text{(AASHTO Eq. 3.12.2.3-1)}$$

where:

L = expansion length (in.)
α = coefficient of thermal expansion (in./in./°F)
$T_{MaxDesign}$ $T_{MinDesign}$ = max./min. temperature range values

The expansion length, *L*, is commonly measured as the distance between joint openings along the centerline of the bridge. The coefficient of thermal expansion is dependent upon the superstructure type: steel, aluminum, concrete, or wood. For concrete structures, AASHTO 5.4.2.2 provides coefficients of thermal expansion for either normal weight or lightweight concrete. Aggregate used in the concrete mix has a direct impact on the concrete's coefficient of thermal expansion (FHWA 2016), with normal weight concrete having a thermal coefficient in the range of 4 to $8x10^{-6}$/°F. Use of limestone and marble aggregates result in a thermal coefficient at the lower limits of this range while chert and quartzite result in a higher thermal coefficient for those concrete mixes (AASHTO 2020).

After the thermal movement range is determined for the joint, an expansion device is then selected to satisfy design requirements. CDOT BDM states in Section 14.4.2 that joints with thermal movement ranges less than 0.75 inches do not require expansion joints at either substructure locations or the end of

approach slabs. If joint movement is expected to be greater than 0.75 inches but less than 2 inches, small movement joints such as asphaltic plugs, silicone seals, elastomeric or foam compression seals, or saw-seal joints are suggested to be used by CDOT. Due to observed performance in past applications, asphaltic plugs are not preferred for use by CDOT due to issues associated with unfavorable asphalt creep and expansion performance. The BDM goes on to state in section 14.4.4 that strip seals shall be used for all new construction where the thermal movement range is expected to be 4 inches or less. If bridge movement is expected to be greater than 4 inches, modular joints are preferred by CDOT. Additionally, finger joints may be used to accommodate moderate to high movement but are not preferred due to routine maintenance being required to unclog the joint.

Procedure A

Procedure A is described as "the historic method that has been used for bridge design" in AASHTO C3.12.2.1. The method, defined in AASHTO 3.12.2.1, uses two climate definitions to determine the design temperature range: moderate or cold. This is determined by the number of freezing days per year, that is, the number of days where the average temperature is less than 32°F. If the number of days where the average temperature is below 32°F is greater than 14, the climate is considered to be cold. Otherwise, the climate is classified as moderate. Identifying the climate the structure is exposed to is required to determine the temperature range in AASHTO Table 3.12.2.1-1. For concrete structures, the temperature range for Moderate environments is 10° to 80°F and for Cold environments the range is 0° to 80°F .

Procedure B

AASHTO section 3.12.2.2 describes Procedure B used to determine the design theoretical thermal movement range of an expansion joint via temperature contour maps developed from historical data. Figures 3.12.2.2-1 and 3.12.2.2-2 in AASHTO are extreme bridge design temperatures for concrete girder bridges with concrete decks based on an average history of 70 years with a minimum of 60 years of data for locations throughout the U.S (AASHTO 2020). By using historical data, a more likely and accurate $T_{MaxDesign}$ and $T_{MinDesign}$ can be used to determine the thermal range compared to Procedure A. Figure 2-1 below shows the temperature contour maps presented in AASHTO 3.12.2.2. The commentary in this section of AASHTO states that when the location of the structure is between contour lines, interpolation or selection of the contour value which results in maximum thermal range may be used (AASHTO 2020). Maximum temperature can be as high as 125°F while the minimum temperature can be taken as low as -55°F, as shown in Figure 2-1.

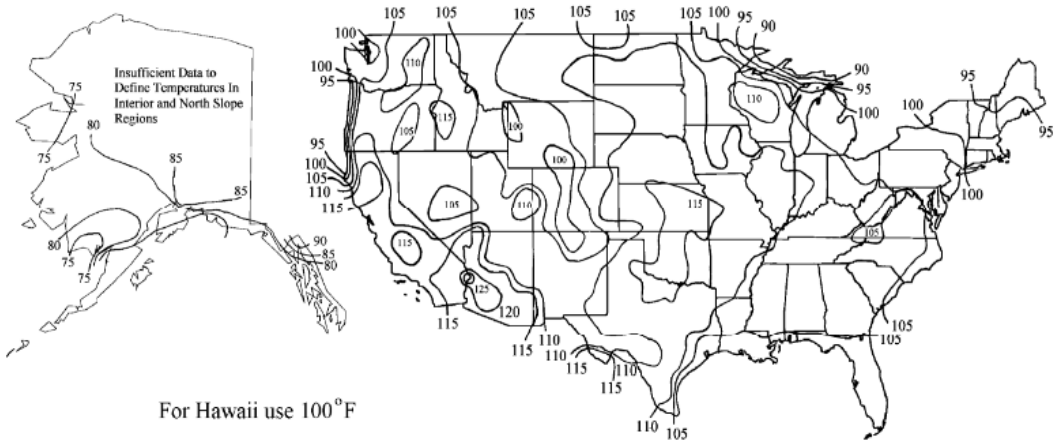

Figure 3.12.2.2-1—Contour Maps for $T_{MaxDesign}$ for Concrete Girder Bridges with Concrete Decks

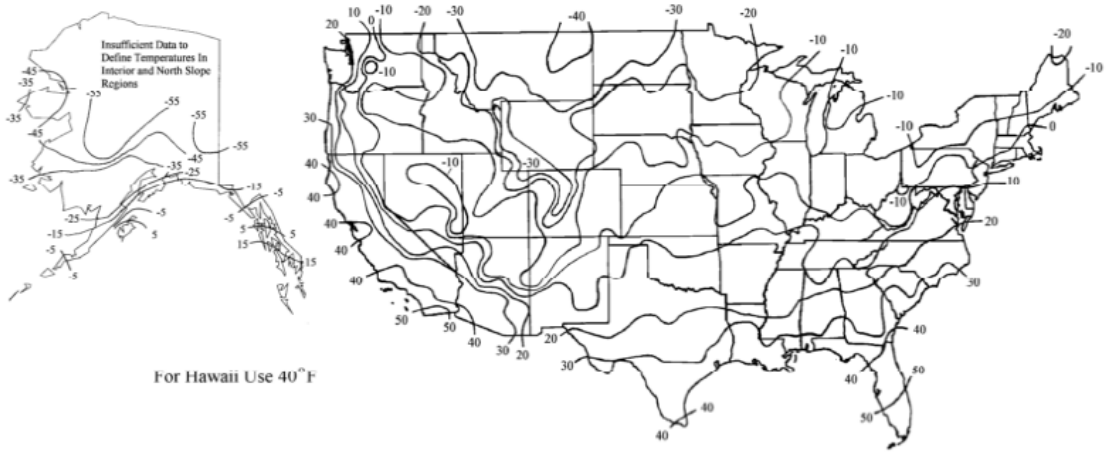

Figure 3.12.2.2-2—Contour Maps for $T_{MinDesign}$ for Concrete Girder Bridges with Concrete Decks

Figure 2-1 AASHTO temperature contour maps (AASHTO 2020)

Bridge Selection and Instrumentation

3.1 Selection Criteria

To collect data representative of the bridges of interest, numerous selection criteria were implemented to identify candidate bridges. Table 3-1contains the criteria used to filter the CDOT bridge database.

Table 3-1 Bridge selection criteria and rationale

Selection Criteria	Rationale and Notes
Integral abutment bridge with prestressed concrete bulb tee girders	Most common and preferred CDOT bridge type
Expansion joints in good working condition	Recently installed, minimal clogging, able to move – allowing for measurement
Bridge components in satisfactory condition	Bridge is in service and shows no signs of settlement/cracking which could affect results
Single, or double span bridges, long span preferred	Simple, long span bridges will provide the most accurate and definitive data per CDOT
No or minimal horizontal skew on bridge	Horizontal skew may cause variable joint translation
No or minimal vertical curve on bridge	Vertical curves may cause uneven joint translation
Bridge joints can be accessed for instrumentation and monitoring	Safely accessible by crew, equipment will not be tampered with
Bridges from various regions of Colorado within reasonable travel distance	Collect data to represent the many climate regions and exposure conditions of Colorado

With the assistance of CDOT personnel and site visits to candidate bridges, eight bridges were selected for instrumentation. These bridges are presented in the following section.

3.2 Overview of Selected Bridges

The bridges listed in Table 3-2 met most, if not all, of the criteria specified in Table 3-1 per site visit observations and review of construction drawings. Two box girder bridges, C-15-Y and F-17-KX, were selected to determine if CBT girder bridges and box girder bridges behave similarly. The box girder bridges also allowed for comparing mountain region temperatures to front range temperatures.

Table 3-2 Summary of selected bridges

Structure Number	Region	County	Mainline	Cross Street/ Feature	Girder Type	Foundation Type	No. of Spans
D-17-FK	4	Weld	SH 66	St. Vrain Creek	CBT	Steel H-Pile	2
C-22-CF	4	Morgan	I76 EB	County Road 29	CBT	Steel H-Pile	1
C-22-CG	4	Morgan	I76 WB	County Road 29	CBT	Steel H-Pile	1
D-04-BOST-170A	1	Denver	Brighton Blvd	Race Ct	CBT	Steel H-Pile	1
DOUHESS 3.35	1	Douglass	Hess Rd	Livestock Crossing	CBT	Steel H-Pile	1
DOUHESS 3.95	1	Douglass	Hess Rd	Newlin Gulch	CBT	Steel H-Pile	1
C-15-Y	4	Larimer	US Hwy 34	Big Thompson River	Box	Drilled Shaft	2
F-17-KX	1	Arapahoe	On Ramp to N Parker Rd	Pedestrian Path	Box	Drilled Shaft	1

Figure 3-1 shows the geographical locations of each bridge.

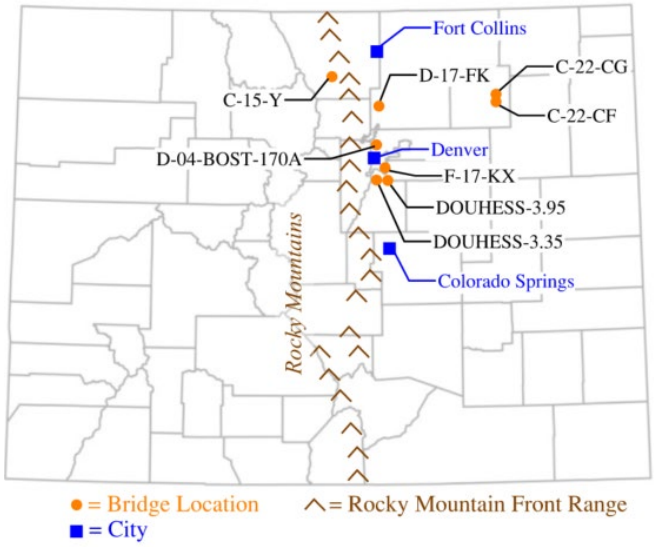

Figure 3-1 Map of Colorado showing bridge locations

An effort was made to select bridges which represent the various exposure conditions present in Colorado while maintaining close proximity to Fort Collins to minimize travel to site time for installation and monitoring. Schematics of each bridge, based on As-Built drawings provided by CDOT, are presented in Appendix A.

3.3 Scratch Gauges

Devices were required to continually record joint translation throughout the study's one year duration. To collect adequate data from each bridge in a practical low-cost manner, a mechanical scratch gauge was implemented at each corner of all selected bridges for a total of 30 scratch gauges (bridge F-17-KX had an inaccessible joint, thus only two gauges were installed). The decision to utilize scratch gauges was driven by cost, installation time, and ease of monitoring. With minimal literature discussing the use or construction of scratch gauges, a prototype gauge was developed and tested for efficacy. The scratch gauge, shown in Figure 3-2, featured a simple three-piece design: composite base, scratch arm and stylus, and scratch plate.

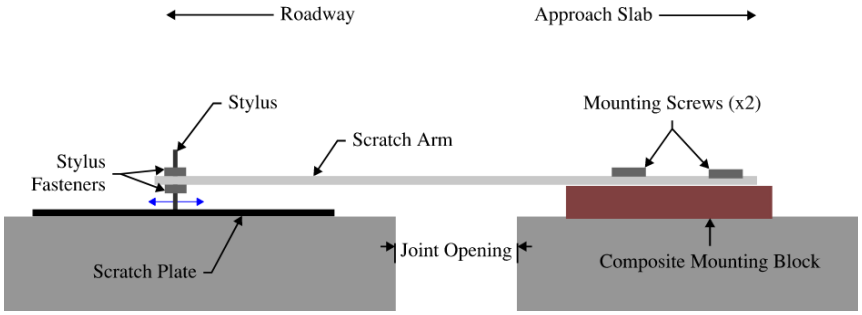

Figure 3-2 Scratch gauge schematic

The composite base sections were sourced from composite deck boards, cut into approximately two-inch-wide pieces. The composite bases were attached to the two sides of the joint using an adhesive, and then screws into the composite base were used to attach the stylus. A composite material was chosen to allow for screws to be attached to the bridge while providing durability under constant weather exposure. The scratch arm was an aluminum bar, durable for consistent outdoor exposure and flexible to allow for stylus setting during installation. The stylus was simply a bolt with the tip filed to a point which scrapes into the scratch plate. The scratch plates were made from sheet metal cut into approximately 3"x8" pieces, roughened to allow for paint primer to bond to the metal surface, and then coated in four layers of outdoor rust-free spray paint. The paint layer was scratched by the stylus as the bridge expanded or contracted, leaving a definitive line which could then be measured to determine the total thermal movement range. Additional information about the S

Before constructing the scratch gauges, a prototype was created and tested for accuracy and effectiveness in a controlled environment using a modified setup for a Universal Testing Machine (UTM), as shown in Figure 3-3.

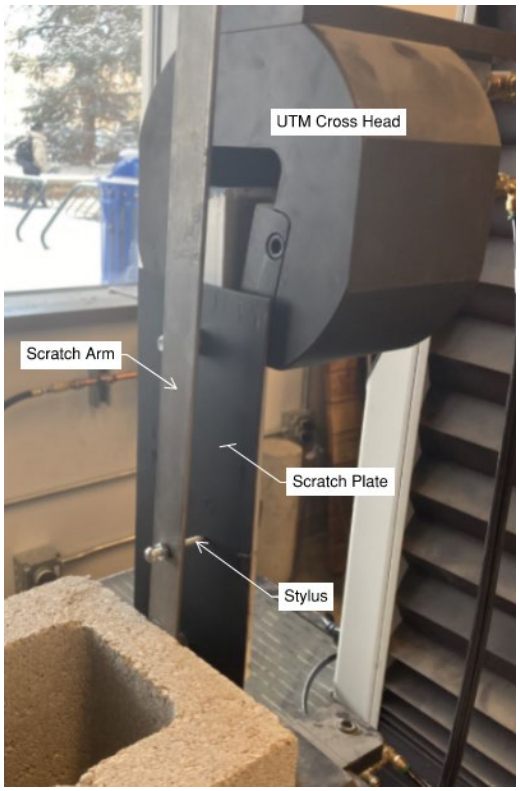

Figure 3-3 Scratch gauge prototype for testing

To conduct the test, the scratch arm and stylus were fixed to a base while a scratch plate was attached to the UTM cross head. The cross head was then slowly raised an inch, then slowly lowered two inches to resemble large bridge movements. The length of scratch was then measured and compared to the actual cross head movement, presented in Table 3-3. The column titled "UTM Reading" was taken after moving the cross head down approximately 2 inches, after having been zeroed at the 1 inch raised position. The length of the scratch on the scratch plate was measured with a digital caliper. This process was repeated for three stylus pressures, controlled by tightening or loosening the stylus nuts and in turn controlling the clamping force the aluminum arm exerts on the stylus indicated by the induced bend from the stylus nut positioning. The three tests included a lightly tightened stylus nut (little bend in the scratch arm), medium tightening (moderate bend in the arm), and hard tightening (high bend in the arm).

Table 3-3 Scratch gauge test results

Test	Force	UTM Reading (in.)	Scratch Length (in.)	Error (in.)	Error (in/in)	Error (%)
1	Light	1.9994	1.986	0.013	0.0067	0.67
2	Medium	2.0031	2.022	0.019	0.0094	0.94
3	Hard	2.0010	1.925	0.076	0.0380	3.80

The scratch gauge prototype test established that a medium tight stylus, or medium force exerted from the stylus onto the scratch plate, resulted in an accurate result and would allow for moderate lateral translation while still maintaining contact with the scratch plate. If the stylus exerts excessive pressure onto the scratch plate, the stylus could bend rather than slide and ultimately damage the gauge while

recording inaccurate data. Conversely, a light stylus pressure could result in loss of contact with the scratch plate throughout the duration of the study if unaccounted for lateral movements occur. It can be seen in Figure 3-4 that the light force stylus scratched the black surface paint but did not penetrate the orange primer below. The medium force stylus score reached the primer while not scratching the metal plate beneath, and the hard force test scratched into the metal plate. While all results are within an accuracy range acceptable for this study, a moderate depth scratch was selected for instrumentation.

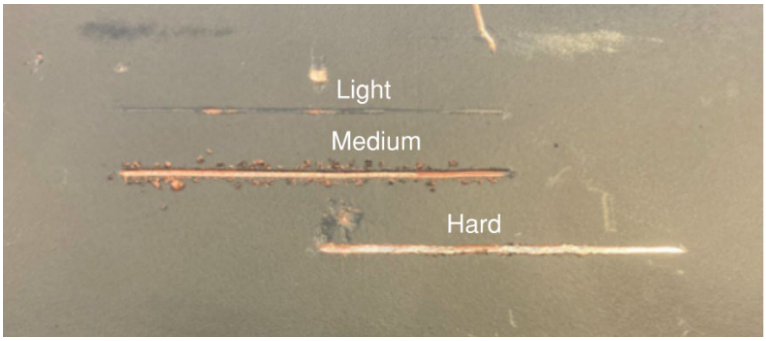

Figure 3-4 Scratches on scratch plate from prototype tests

In order to attach both the scratch plate and composite base to the concrete bridge surfaces, an industrial adhesive, Loctite PL Premium MAX Construction Adhesive, was selected based on a cure time of 20 minutes, strength for industrial applications, and durability in exposed environments. More on the scratch gauge installation can be found in Section 3.5.

3.4 Electrical Sensors

In addition to mechanical sensors affixed to all study bridges, two bridges were equipped with electrical sensors to measure movement and temperature on an hourly interval. These gauges were used to not only validate the mechanical sensors, but to also gather more accurate temperature and movement data. The two bridges selected for electrical instrumentation, C-22-CF and D-17-FK, allowed for easy access to and from the Colorado State University campus and were both longer span structures with minimal to no vertical grade, allowing for the most accurate and substantial measurement of thermal effects on the structure.

3.4.1 Displacement Sensors

Two electrically equipped potentiometers were attached at both sides of the expansion joint at one end of the selected bridge. Similar to the scratch gauges, composite board was used as a mounting base on either side of the joint to which the potentiometer and an eye bolt were attached. Potentiometers function by reading an input voltage dependent upon the position of the head. The measured voltage values are then converted into unit measurements which can be analyzed to determine maximum and minimum positions of the head. Gefran 130mm potentiometer linear position sensors were used to collect hourly voltage values, which were then stored in a data acquisition system (DAQ) for retrieval and monitoring throughout the study. Figure 3-5 shows the potentiometer attached to a bridge with the head securely fastened to an eye bolt on the opposite side of the joint.

Figure 3-5 Installed potentiometer linear position sensor

3.4.2 Temperature Sensors

In addition to potentiometers, the bridges selected for electrical instrumentation were also equipped with a 12-Bit Temperature Smart Sensors from ONSET to record hourly temperature readings to be compared to local weather stations and the temperature ranges presented in AASHTO. Additionally, mountain bridge C-15-Y was equipped with two Monarch Track-It Temperature Data Loggers, positioned on the east and west ends of the bridge to also compare hourly temperature values to local weather station data and AASHTO temperature ranges. While the 12-Bit Temperature sensors required a DAQ setup and energy supply, the Monarch sensors were battery powered and USB accessible for ease of data collection and minimal setup required. Both types of sensors were placed to avoid direct sun exposure. The ONSET sensors were placed in the shade of the solar panel, and the Monarch loggers were hung from the side of the bridge. Figure 3-6 shows the two temperature sensors used in this study.

(a)

(b)

Figure 3-6 Temperature loggers (a) 12-Bit Temperature Smart Sensors and (b) Monarch Track-It Temperature Data Loggers

3.4.3 Data Acquisition System and Power Source

To record and store the data from the potentiometers and temperature loggers, a DAQ was implemented with a continual 5-watt solar power supply. A HOBO U30 USB Weather Station Data Logger was selected due to its ability to store data from two potentiometers and the temperature logger simultaneously at each electrically equipped bridge. Data stored in the DAQ can be accessed through a micro-USB port connected to a portable device while using the HOBOware software specifically designed for the HOBO weather station products.

3.5 Gauge Installation

With gauges and materials acquired and prepared for installation, the bridges were instrumented to record thermal movements and temperatures throughout the study's 15-month duration. Figure 3-7 shows, in plan-view, the instrumentation scheme used at all bridges for the scratch gauges along with sensor staging for the two electronically instrumented bridges. As shown via the orange line, the potentiometers required a wired connection to the DAQ for power supply and data transmission. Therefore, the wire was run along the bridge abutment under the bridge to avoid damage from vehicle traffic above and minimize potential threat or damage to and from wildlife.

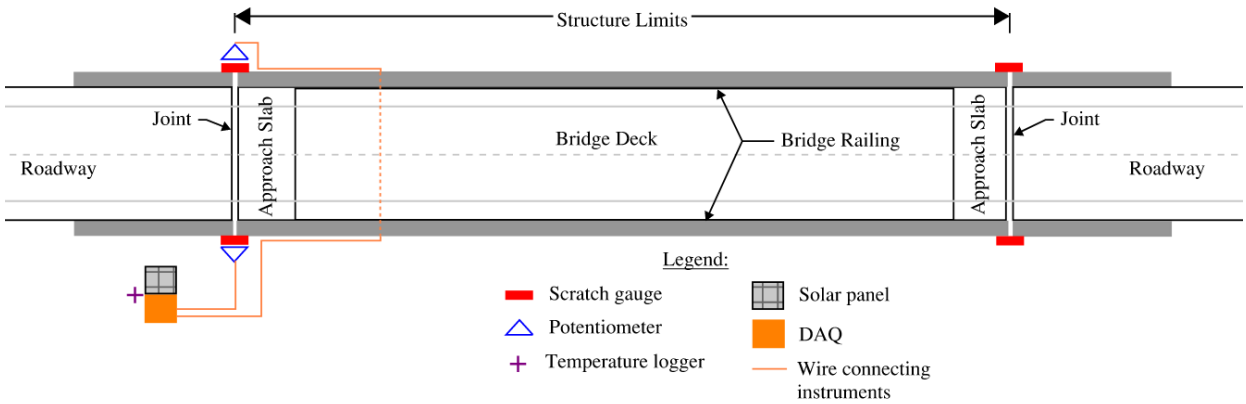

Figure 3-7 Bridge instrumentation schematic

The first step of scratch gauge installation was using an even layer of adhesive to attach the mounting blocks and scratch plates to the bridge structures. The adhesive was also used to provide extra support for the connection between the scratch arm and mounting block and was utilized on all screw, bolt, and nut threads to ensure a durable connection and avoid loose or unstable parts of the scratch gauges. The scratch gauges were installed over two days to allow ample time for the adhesive to cure before mounting the scratch arm. Thus, scratch plates and mounting bases were fastened to all structures on the first day and scratch arm and stylus attached the following day. Figure 3-8 shows an installed scratch gauge.

Figure 3-8 Scratch gauge installed on a bridge

The electrical sensors were attached and wired to the DAQ in one day to ensure all systems were working properly with the lab technician present who was assisting on the project. A weatherproof cover consisting of a PVC pipe cut in half and attached to one half of the bridge joint provided added protection to the potentiometers from weather elements and potential snow drifts in winter months. By attaching the PVC to only one half of the joint, relative movement between the two sides was uninhibited, while still providing protection to the instrumentation. Figure 3-9 and Figure 3-10 display the electrical sensors and DAQ system installed on site.

Figure 3-9 Equipped Potentiometer with weatherproofing installed

Figure 3-10 DAQ as installed on-site with solar panel

Instrumentation was left in place for over one year to capture joint movement as the bridge was exposed to seasonal temperature variations.

Theoretical Movement Calculations

CDOT Provisions

CDOT prefers theoretical thermal bridge movement to be calculated using temperatures defined in Procedure B of the AASHTO LRFD Bridge Design Code, but may also accept Procedure A and Temperature Gradient methods where appropriate. The Temperature Gradient method presented in AASHTO 3.12.3 is used when differential thermal movement across the structure's height is of interest. Differential movements across the depth of a bridge result in bending deformation, which was not the focus of this study and was not a type of movement the gauges and instruments were selected to measure. Thus, as the Temperature Gradient method is not a preferred CDOT design procedure, and is outside the focus of the study the Temperature Gradient was not considered.

AASHTO Methods for Prediction of Thermal Movement

The governing equation for the design thermal movement range of a structure for both Procedure A and Procedure B is AASHTO Eq 3.12.2.3-1:

$$\Delta_T = \alpha L(T_{MaxDesign} - T_{MinDesign})$$

A common parameter in both procedures is the coefficient of thermal expansion, α. For normal weight concrete structures, which applies to all bridges analyzed in this study, the coefficient of thermal expansion is $6x10^{-6}/°F$ per AASHTO 5.4.2.2.

Next, the expansion length, *L*, must be determined for each structure. Moreover, the expansion length each joint will be designed to tolerate must be determined. This input is unique to each bridge, and is the variable in AASHTO Eq. 3.12.2.3-1 that had the largest impact on the thermal design movement range. The expansion length was calculated using the As-Built drawings for each bridge provided by CDOT (schematics in Appendix A). The expansion length, *L*, for each joint was calculated by adding half the structure length plus the approach slab length, as summarized in Table 4-1.

Table 4-1 Expansion lengths of each bridge

Structure Number	Structure Length (BF Abut - BF Abut) (ft)	East Approach Slab Length (Exp Joint - BF Abut) (ft)	West Approach Slab Length (Exp Joint - BF Abut) (ft)	East Expansion Length (ft)	West Expansion Length (ft)
D-17-FK	265.50	20.00	20.00	152.75	152.75
C-22-CF	131.00	25.00	25.00	90.50	90.50
C-22-CG	131.00	25.00	25.00	90.50	90.50
D-04-BOST-170A	92.67	20.00	15.00	66.33	61.33
DOUHESS 3.35	92.00	20.00	20.00	66.00	66.00
DOUHESS 3.95	71.00	20.00	20.00	55.50	55.50
C-15-Y	145.50	20.00	20.00	92.75	92.75
F-17-KX	59.24	19.69	N.A.	49.30	N.A.

By inspection, it is anticipated that the joints on bridge D-17-FK will experience the largest thermal movement range as this bridge has the longest expansion lengths among selected bridges. Conversely, bridge F-17-KX among box girder bridges and bridge DOUHESS 3.95 among CBT bridges are expected to display the lowest thermal movement range due to having the shortest expansion length among selected bridges.

The load factors for effects due to temperature, γ_{TU}, are found in AASHTO Table 3.4.1-1. There are two load factors listed for effects due to temperature, *TU*. For Strength limit states, the load factors are 0.5 and 1.2. For Service limit states, the load factors are 1.0 and 1.2. AASHTO 3.4.1 states "The larger of the two values provided for load factor of TU shall be used for deformations and the smaller values for all other effects." The commentary also states a load factor greater than 1.0 is utilized to avoid under-sizing joints, expansive devices, and bearings. For the purposes of this study, theoretical movements were calculated using a minimum load factor of γ_{TU_min}=1.00 and a maximum load factor of γ_{TU_max}=1.20 in order to compare both theoretical values to measured movements. The load factors are applied after Δ_T is calculated per Eq. 3.12.2.3-1 to determine the total theoretical movement at the joint.

The remaining inputs for Eq 3.12.2.3-1 are the temperature range values. The following sections determine the temperature range of each bridge for Procedure A and Procedure B.

Procedure A Bridge Movements

As described in Section 2.3.1.1 , Procedure A specifes a tempertaure range based on the construction material of the bridge and climate type (either moderate or cold). The normal average temperature for January in Denver, Colorado is 31.7°, so there are more than 14 days per year with an average temperature below 32°F (National Weather Service n.d.). This classifies the Denver area as a cold climate per AASHTO C3.12.2.1, which will be used for all bridges in this study as they are in close proximity and metropolitan areas tend to have higher average temperatures than surrounding rural areas (EPA 2023). The design temperature range used in this study for Procedure A is 0°F-80°F.

Using the expansion lengths in Table 4-1, the theoretical bridge movements for each study bridge per AASHTO Procedure A and Eq. 3.12.2.3-1 are summarized in Table 4-2.

Table 4-2 Procedure A theoretical bridge movements

Structure Number	Joint	Expansion Length (ft)	Tmax (AASHTO Table 3.12.2.1-1) (°F)	Tmin (AASHTO Table 3.12.2.1-1) (°F)	Calc. Movement γ_{TU}=1.00 (in.)	Calc. Movement γ_{TU}=1.20 (in)
D-17-FK	East	152.75	80	0	0.880	1.056
D-17-FK	West	152.75	80	0	0.880	1.056
C-22-CF	East	90.50	80	0	0.521	0.626
C-22-CF	West	90.50	80	0	0.521	0.626
C-22-CG	East	90.50	80	0	0.521	0.626
C-22-CG	West	90.50	80	0	0.521	0.626
D-04-BOST-170A	East	66.33	80	0	0.382	0.458
D-04-BOST-170A	West	61.33	80	0	0.353	0.424
DOUHESS 3.35	East	66.00	80	0	0.380	0.456
DOUHESS 3.35	West	66.00	80	0	0.380	0.456
DOUHESS 3.95	East	55.50	80	0	0.320	0.384
DOUHESS 3.95	West	55.50	80	0	0.320	0.384
C-15-Y	East	92.75	80	0	0.534	0.641
C-15-Y	West	92.75	80	0	0.534	0.641
F-17-KX	East	49.30	80	0	0.284	0.341

Procedure B Bridge Movements

In contrast to Procedure A, Procedure B uses contour maps for temperature as described in Section 2.3.1.2 . To determine the minimum and maximum design temperature for Procedure B, the location of each bridge must be determined on the temperature contour maps in AASHTO 3.12.2.2. For concrete girder bridges with concrete decks, AASHTO Fig. 3.12.2.2-1 is used to determine $T_{MaxDesign}$ and AASHTO Fig. 3.12.2.2-2 is used to determine $T_{MinDesign}$. To aid in reading these maps, the bridges and their respective location were plotted on the contour maps as shown in Figure 4-1 and Figure 4-2:

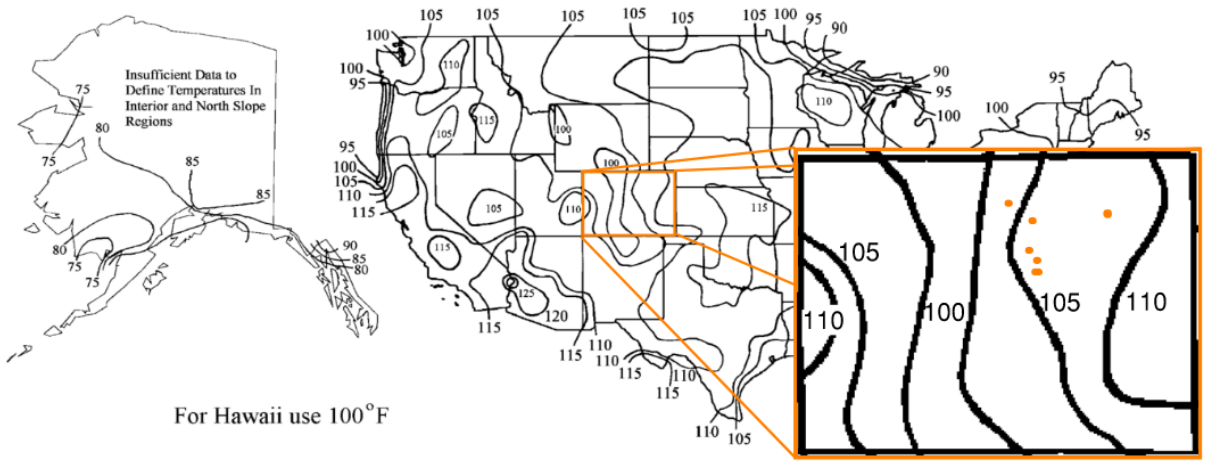

Figure 3.12.2.2-1—Contour Maps for $T_{MaxDesign}$ for Concrete Girder Bridges with Concrete Decks

Figure 4-1 AASHTO contour map for high temperatures with bridge location detail

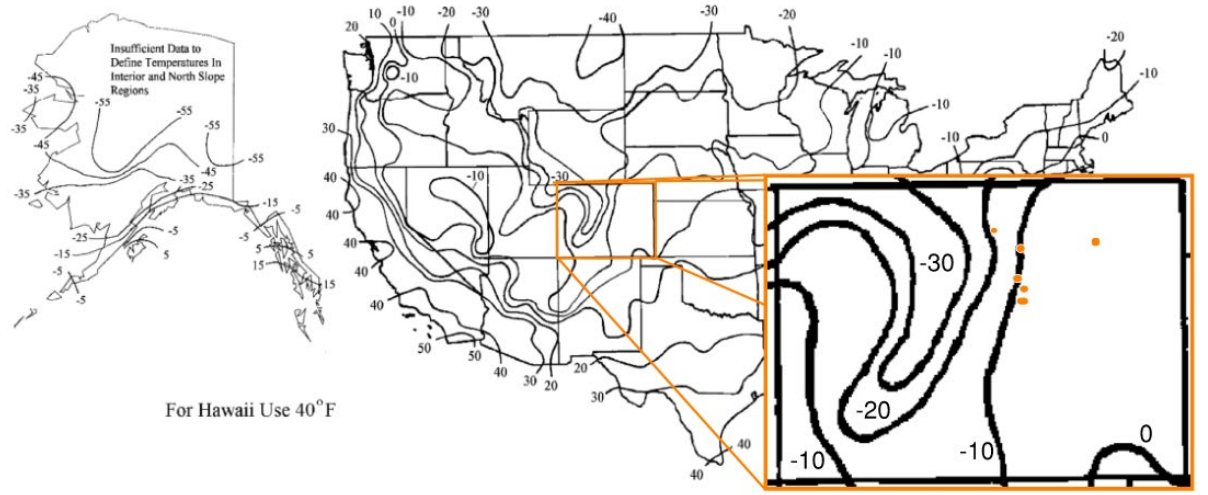

Figure 3.12.2.2-2—Contour Maps for $T_{MinDesign}$ for Concrete Girder Bridges with Concrete Decks

Figure 4-2 AASHTO contour map for low temperatures with bridge location detail

Per AASHTO C3.12.2.2, "The design values for locations between contours should be determined by linear interpolation. As an alternative method, the largest adjacent contour may be used to define $T_{MaxDesign}$ and the smallest adjacent contour may be used to define $T_{MinDesign}$." The controlling contour values from Figure 4-1and Figure 4-2and the theoretical bridge movements per AASHTO Procedure B and Eq. 3.12.2.3-1 are summarized in Table 4-3.

Table 4-3 Procedure B theoretical bridge movements

Structure Number	Joint	Expansion Length (ft)	Tmax (AASHTO Fig. 3.12.2.2-1) (°F)	Tmin (AASHTO Fig. 3.12.2.2-2) (°F)	Calc. Movement γ_{TU}=1.00 (in.)	Calc. Movement γ_{TU}=1.20 (in.)
D-17-FK	East	152.75	105	-10	1.265	1.518
D-17-FK	West	152.75	105	-10	1.265	1.518
C-22-CF	East	90.50	110	-10	0.782	0.938
C-22-CF	West	90.50	110	-10	0.782	0.938
C-22-CG	East	90.50	110	-10	0.782	0.938
C-22-CG	West	90.50	110	-10	0.782	0.938
D-04-BOST-170A	East	66.33	105	-10	0.549	0.659
D-04-BOST-170A	West	61.33	105	-10	0.508	0.609
DOUHESS 3.35	East	66.00	105	-10	0.546	0.656
DOUHESS 3.35	West	66.00	105	-10	0.546	0.656
DOUHESS 3.95	East	55.50	105	-10	0.460	0.551
DOUHESS 3.95	West	55.50	105	-10	0.460	0.551
C-15-Y	East	92.75	105	-20	0.835	1.002
C-15-Y	West	92.75	105	-20	0.835	1.002
F-17-KX	East	49.30	105	-10	0.408	0.490

Theoretical movements for AASHTO Procedure A and Procedure B are compared to observed bridge movement in Section 5.5 to determine accuracy and efficacy of each procedure.

Joint Classification

Table 4-4 shows that Procedure A consistently predicts a smaller design thermal movement range when compared to Procedure B. This is due to a more refined temperature range used in Procedure B, where the contour maps are created using collected data (AASHTO 2020) as opposed to designing for a general climate per Procedure A.

Table 4-4 Comparison of theoretical bridge movement calculations

Structure Number	Joint	Procedure A Calc. Movement γ=1.00 (in)	Procedure A Calc. Movement γ=1.20 (in.)	Procedure B Calc. Movement γ=1.00 (in.)	Procedure B Calc. Movement γ=1.20 (in.)	$\Delta_{\gamma\text{-min}}$ Pro.B - Pro.A (in.)	$\Delta_{\gamma\text{-max}}$ Pro.B - Pro.A (in.)
D-17-FK	East	0.880	1.056	1.265	1.518	0.385	0.462
D-17-FK	West	0.880	1.056	1.265	1.518	0.385	0.462
C-22-CF	East	0.521	0.626	0.782	0.938	0.261	0.313
C-22-CF	West	0.521	0.626	0.782	0.938	0.261	0.313
C-22-CG	East	0.521	0.626	0.782	0.938	0.261	0.313
C-22-CG	West	0.521	0.626	0.782	0.938	0.261	0.313
D-04-BOST-170A	East	0.382	0.458	0.549	0.659	0.167	0.201
D-04-BOST-170A	West	0.353	0.424	0.508	0.609	0.155	0.185
DOUHESS-3.35	East	0.380	0.456	0.546	0.656	0.166	0.200
DOUHESS-3.35	West	0.380	0.456	0.546	0.656	0.166	0.200
DOUHESS-3.95	East	0.320	0.384	0.460	0.551	0.140	0.168
DOUHESS-3.95	West	0.320	0.384	0.460	0.551	0.140	0.168
C-15-Y	East	0.534	0.641	0.835	1.002	0.301	0.361
C-15-Y	West	0.534	0.641	0.835	1.002	0.301	0.361
F-17-KX	East	0.284	0.341	0.408	0.490	0.124	0.149
					Average:	0.231	0.278

The temperature design range is the controlling difference between the two procedures. Procedure A recommends a thermal range of 80°F while Procedure B specifies a design range of up to 120°F for the same structures. This temperature difference directly impacts the design thermal movement range, Δ_T, as shown in Table 4-4. Depending on the structure, Procedure A predicts a thermal movement range 30%-36% less than that predicted by Procedure B, which for this set of bridges results in a 0.140 - 0.462 inch smaller thermal design range. The accuracy of each procedure in predicting thermal movements for the selected bridges will be discussed in Section 5.5 .

Regardless of expected thermal movement range, the CDOT BDM requires strip seal joints for all new construction, which was abided by as each selected bridge uses strip seal joints as expansion devices. This may be unnecessary where expected bridge movement is less than 0.75 inches as calculated per Procedure B with the maximum load factor applied such as for bridges D-04-BOST-170A, DOUHESS-3.35, DOUHESS-3.95, C-15-Y, and F-17-KX . A small movement joint, applicable for movements less than 0.75 inches, may have been more applicable and cost effective for these bridges per the calculated movements shown in Table 4-4.

Results and Discussion

Scratch Gauge Results

After approximately 15 months of data collection, each scratch gauge was observed to determine the magnitude of movement each joint experienced. The length of scratch on each gauge was measured on site using a ruler, as shown in Figure 5-1. The gauges were left in place on the bridges to allow CDOT to continue monitoring bridge movement.

Figure 5-1 Scratch gauge measurement

Table 5-1 summarizes the scratch gauge measurements for each bridge. The Measured Movement is the total range of movement the bridge underwent during the 15 months of the study. As gauges were placed in the spring, the scratch extended in one direction from the original stylus placement during the summer as the bridge expanded during hot summer temperatures, and then moved back in the other direction as the bridge contracted during cold winter temperatures to create the total length. Scratch gauges were placed on both ends of each joint, and the Average Measured Movement column shows the average of the range of movement on the two ends.

Table 5-1 Bridge joint movement measured from scratch gauges

Structure Number	Joint	Corner	Measured Movement (in.)			Average Measured Movement (in.)
D-17-FK	East	NE	11/16	=	0.688	0.688
D-17-FK	East	SE	11/16	=	0.688	0.688
D-17-FK	West	NW	12/16	=	0.750	0.719
D-17-FK	West	SW	11/16	=	0.688	0.719
C-22-CF	East	NE	13/16	=	0.813	0.781
C-22-CF	East	SE	12/16	=	0.750	0.781
C-22-CF	West	NW	11/16	=	0.688	0.688
C-22-CF	West	SW	11/16	=	0.688	0.688
C-22-CG	East	NE	14/16	=	0.875	0.875
C-22-CG	East	SE	14/16	=	0.875	0.875
C-22-CG	West	NW	11/16	=	0.688	0.750
C-22-CG	West	SW	13/16	=	0.813	0.750
D-04-BOST-170A	East	NE	6/16	=	0.375	0.344
D-04-BOST-170A	East	SE	5/16	=	0.313	0.344
D-04-BOST-170A	West	NW	5/16	=	0.313	0.344
D-04-BOST-170A	West	SW	6/16	=	0.375	0.344
DOUHESS 3.35	East	NE	9/16	=	0.563	0.531
DOUHESS 3.35	East	SE	8/16	=	0.500	0.531
DOUHESS 3.35	West	NW	8/16	=	0.500	0.469
DOUHESS 3.35	West	SW	7/16	=	0.438	0.469
DOUHESS 3.95	East	NE	5/16	=	0.313	0.344
DOUHESS 3.95	East	SE	6/16	=	0.375	0.344
DOUHESS 3.95	West	NW	8/16	=	0.500	0.500
DOUHESS 3.95	West	SW	8/16	=	0.500	0.500
C-15-Y	East	NE	9/16	=	0.563	0.500
C-15-Y	East	SE	7/16	=	0.438	0.500
C-15-Y	West	NW	7/16	=	0.438	0.344
C-15-Y	West	SW	4/16	=	0.250	0.344
F-17-KX	East	NE	6/16	=	0.375	0.406
F-17-KX	East	SE	7/16	=	0.438	0.406

Table 5-1 shows the majority of gauges on common joints recorded similar movement (within 1/16 of an inch), but some had larger discrepancies, such as the West joint on C-15-Y where the difference between joint ends was 3/16 inch. This variance in movement on the opposite ends of the same joint is likely a result of clogging or restriction of movement along the joint. These differential movements observed on a

common joint can cause additional stresses in the adjoining bridge approach slab and roadway resulting in expansion system damage observable through cracked pavement around the joint.

Temperature Sensor Results

Data from bridges equipped with a temperature sensor were analyzed and the maximum and minimum recorded temperatures were compared with local weather station data and AASHTO Procedure B temperature range maps. Local weather station data was accessed via the National Oceanic and Atmospheric Administration (NOAA) database on weather.gov (National Weather Service). Table 5-2summarizes the maximum and minimum temperature ranges observed during the study and compares these ranges to the AASHTO values for bridge design.

Table 5-2 Comparison of observed temperature ranges to AASHTO values

Bridge	Nearest Weather Station	Temp. Sensor Min	Temp Sensor Max	Weather Station Min	Weather Station Max	AASHTO Min	AASHTO Max
DOUHESS 3.35, DOUHESS 3.95	Castle Rock, CO	-	-	-14	102	-10	105
F-17-KX, D-04-BOST-170A	Denver Area	-	-	-11	101	-10	105
C-22-CF, C-22-CG	Greeley, CO	-7.99	119.00	-18	106	-10	110
D-17-FK	Longmont, CO	-	-	-15	102	-10	105
C-15-Y	Loveland, CO	29	109	-21	107	-20	105

Comparing local weather station data to the temperatures read from the maps provided in AASHTO shows that the temperatures are generally similar, with a maximum difference between weather station data and AASHTO of 4°F in Greeley, CO and the associated bridges. Minor differences such as this are one of the sources of variability accounted for in the temperature factor of 1.20 applied to theoretical movement calculations per AASHTO.

Potentiometer Results

Data from the temperature sensor and potentiometers equipped to bridge C-22-CF are presented in Figure 5-2. (The DAQ on D-17-FK was found to be not functional after over a year in service, so only C-22-CF data are available.) As expected and shown, the joint opening is directly correlated to the environmental temperature, with the minimum joint opening occurring at maximum temperatures while the largest joint openings occur at low temperatures.

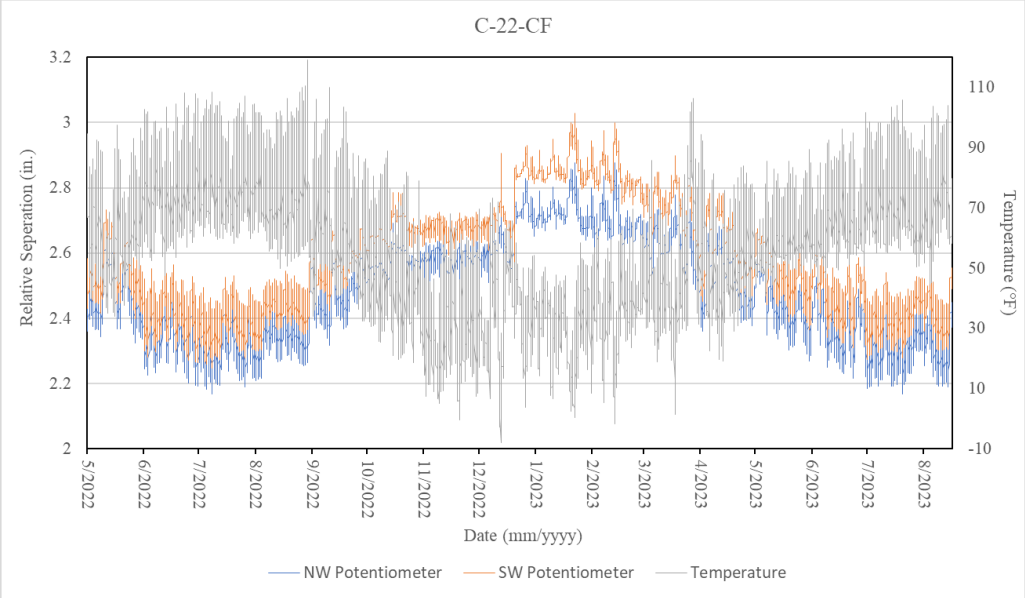

Figure 5-2 Bridge C-22-CF potentiometer and temperature data

Bridge C-22-CF potentiometer data shows that the West joint experienced 0.726 inches and 0.781 inches for the Southwest and Northwest joints respectively while the temperature ranged from -7.99°F to 119.00°F.

Comparison of Mechanical and Electrical Gauge Results

One of the main purposes of equipping bridges with potentiometers was to confirm the efficacy of the scratch gauges implemented on all of the bridges. Table 5-3 compares the thermal movement ranges recorded by potentiometers and scratch gauges to ensure the values are within an acceptable tolerance of each other.

Table 5-3 Scratch gauge results compared to potentiometer readings for bridge C-22-CF

Bridge	Joint	Corner	Min. Separation (in.)	Max Separation (in.)	Movement (in.)	Scratch Gauge (in.)
C-22-CF	West	NW	2.247	3.028	0.781	0.688
C-22-CF	West	SW	2.168	2.895	0.726	0.688

Based on these limited data, the scratch gauges appear to slightly underestimate the total joint movement. The scratch gauge and potentiometer data differ by less than 0.10 inches, which is within reason for the purpose of this study. The potentiometer is expected to be accurate within 0.006 inches within controlled temperature conditions. Comparing the effect of temperature change on the scratch gauges and potentiometer would require focused study with additional data in more controlled conditions.

Comparison of Theoretical Results and Field Data

With theoretical thermal movements calculated and scratch gauge data collected, the values were then compared to determine accuracy and appropriateness of both AASHTO design procedures. Although CDOT prefers the use of Procedure B when determining the thermal movement range, the results presented in Table 5-4 and Table 5-5 include values from both Procedure A and Procedure B to determine the most appropriate method based on the data.

Table 5-4 Scratch gauge measured movement vs. Procedure A theoretical movement

Structure Number	**Joint**	**Measured Movement** (in.)	**Calc. Movement** γ TU min (in.)	**Calc. Movement** γ TU max (in.)	**Difference** (Measured - Calc) (in.)	**Difference** (Measured - Calc) (in.)	**Difference as % of Expansion Length**	**Difference as % of Expansion Length**
D-17-FK	East	0.688	0.88	1.056	-0.192	-0.368	-0.010%	-0.020%
D-17-FK	West	0.719	0.88	1.056	-0.161	-0.337	-0.009%	-0.018%
C-22-CF	East	0.781	0.521	0.626	0.26	0.155	0.024%	0.014%
C-22-CF	West	0.688	0.521	0.626	0.167	0.062	0.015%	0.006%
C-22-CG	East	0.875	0.521	0.626	0.354	0.249	0.033%	0.023%
C-22-CG	West	0.75	0.521	0.626	0.229	0.124	0.021%	0.011%
D-04-BOST-170A	East	0.344	0.382	0.458	-0.038	-0.114	-0.005%	-0.014%
D-04-BOST-170A	West	0.344	0.353	0.424	-0.009	-0.08	-0.001%	-0.011%
DOUHESS 3.35	East	0.531	0.38	0.456	0.151	0.075	0.019%	0.009%
DOUHESS 3.35	West	0.469	0.38	0.456	0.089	0.013	0.011%	0.002%
DOUHESS 3.95	East	0.344	0.32	0.384	0.024	-0.04	0.004%	-0.006%
DOUHESS 3.95	West	0.5	0.32	0.384	0.18	0.116	0.048%	0.058%
C-15-Y	East	0.5	0.534	0.641	-0.034	-0.141	-0.003%	-0.013%
C-15-Y	West	0.344	0.534	0.641	-0.19	-0.297	-0.017%	-0.027%
17-KX	East	0.406	0.284	0.341	0.122	0.065	0.021%	0.011%

Table 5-4 shows that Procedure A may result in under-sizing the joint, seen by the positive difference in measured movement and theoretical movement. Undersizing of a joint is undesirable as it may lead to damage to the structure if the joint cannot accommodate the full range of movement and this data validates CDOT's disposition to not use Procedure A when determining thermal movement ranges.

Figure 5-3 presents the relationship between Procedure A theoretical and measured movements graphically.

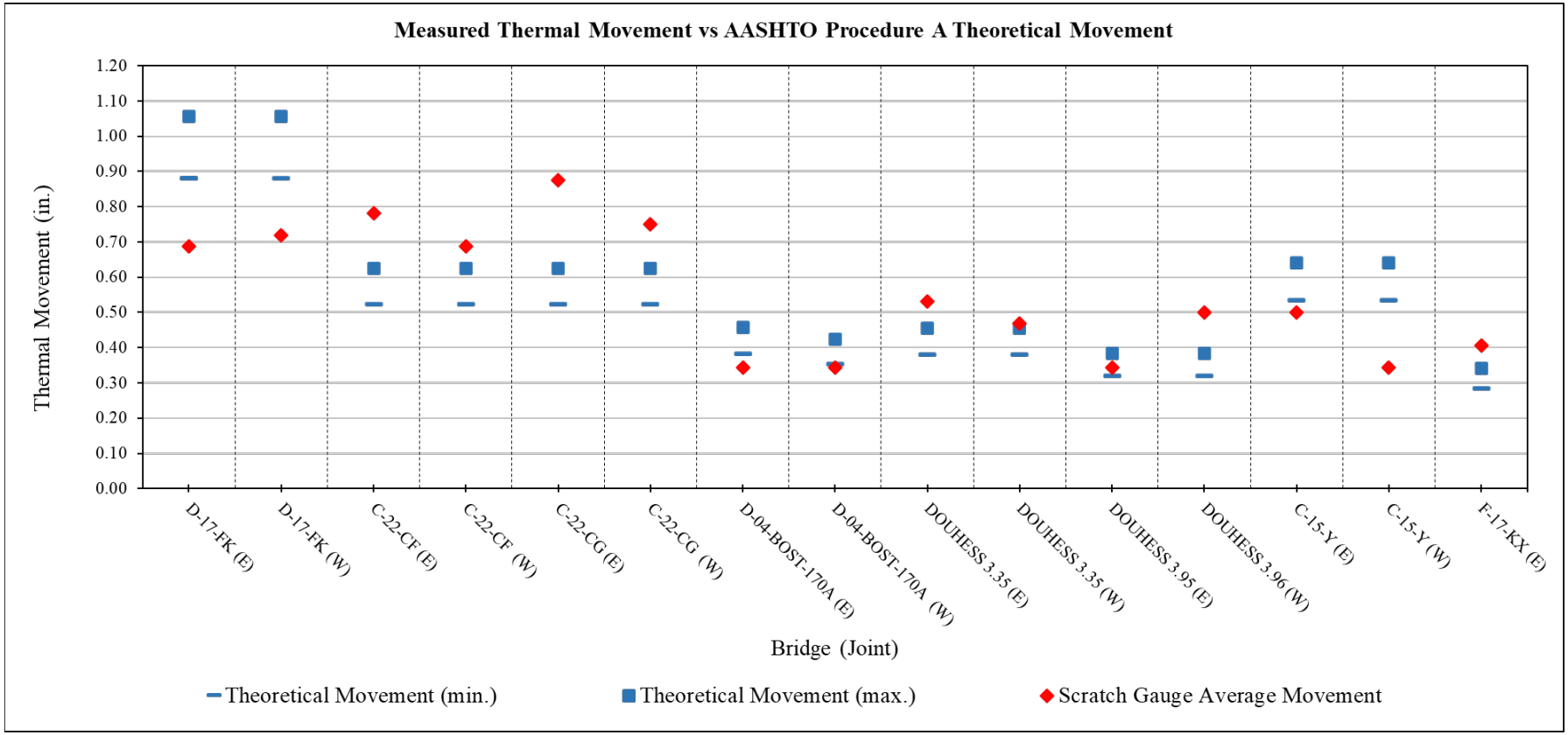

Figure 5-3 Procedure A theoretical movement compared to observed movement

Table 5-5 compares CDOT's preferred method of analysis, Procedure B, to observed movement.

Table 5-5 Scratch gauge measured movement vs. Procedure B theoretical movement

Structure Number	Joint	Measured Movement (in.)	Calc. Movement γ TU min (in.)	Calc. Movement γ TU max (in.)	Difference (Measured-Calc) (in)	Difference (Measured-Calc) (in.)	Difference as % of Expansion Length	Difference as % of Expansion Length
D-17-FK	East	0.688	1.265	1.518	-0.577	-0.83	-0.031%	-0.045%
D-17-FK	West	0.719	1.265	1.518	-0.546	-0.799	-0.030%	-0.044%
C-22-CF	East	0.781	0.782	0.938	-0.001	-0.157	0.000%	-0.014%
C-22-CF	West	0.688	0.782	0.938	-0.094	-0.25	-0.009%	-0.023%
C-22-CG	East	0.875	0.782	0.938	0.093	-0.063	0.009%	-0.006%
C-22-CG	West	0.75	0.782	0.938	-0.032	-0.188	-0.003%	-0.017%
D-04-BOST-170A	East	0.344	0.549	0.659	-0.205	-0.315	-0.026%	-0.040%
D-04-BOST-170A	West	0.344	0.508	0.609	-0.164	-0.265	-0.022%	-0.036%
DOUHESS 3.35	East	0.531	0.546	0.656	-0.015	-0.125	-0.002%	-0.016%
DOUHESS 3.35	West	0.469	0.546	0.656	-0.077	-0.187	-0.010%	-0.024%
DOUHESS 3.95	East	0.344	0.46	0.551	-0.116	-0.207	-0.017%	-0.031%
DOUHESS 3.95	West	0.5	0.46	0.551	0.04	-0.051	0.069%	0.083%
C-15-Y	East	0.5	0.835	1.002	-0.335	-0.502	-0.030%	-0.045%
C-15-Y	West	0.344	0.835	1.002	-0.491	-0.658	-0.044%	-0.059%
F-17-KX	East	0.406	0.408	0.49	-0.002	-0.084	0.000%	-0.014%

As shown in the "Difference" columns of Table 5-5, particularly the far-right column comparing values using the recommended joint sizing load factor of 1.20, Procedure B overpredicts joint movement for all analyzed bridges. Figure 5-4 shows the comparison between AASHTO Procedure B theoretical values and observed movement graphically.

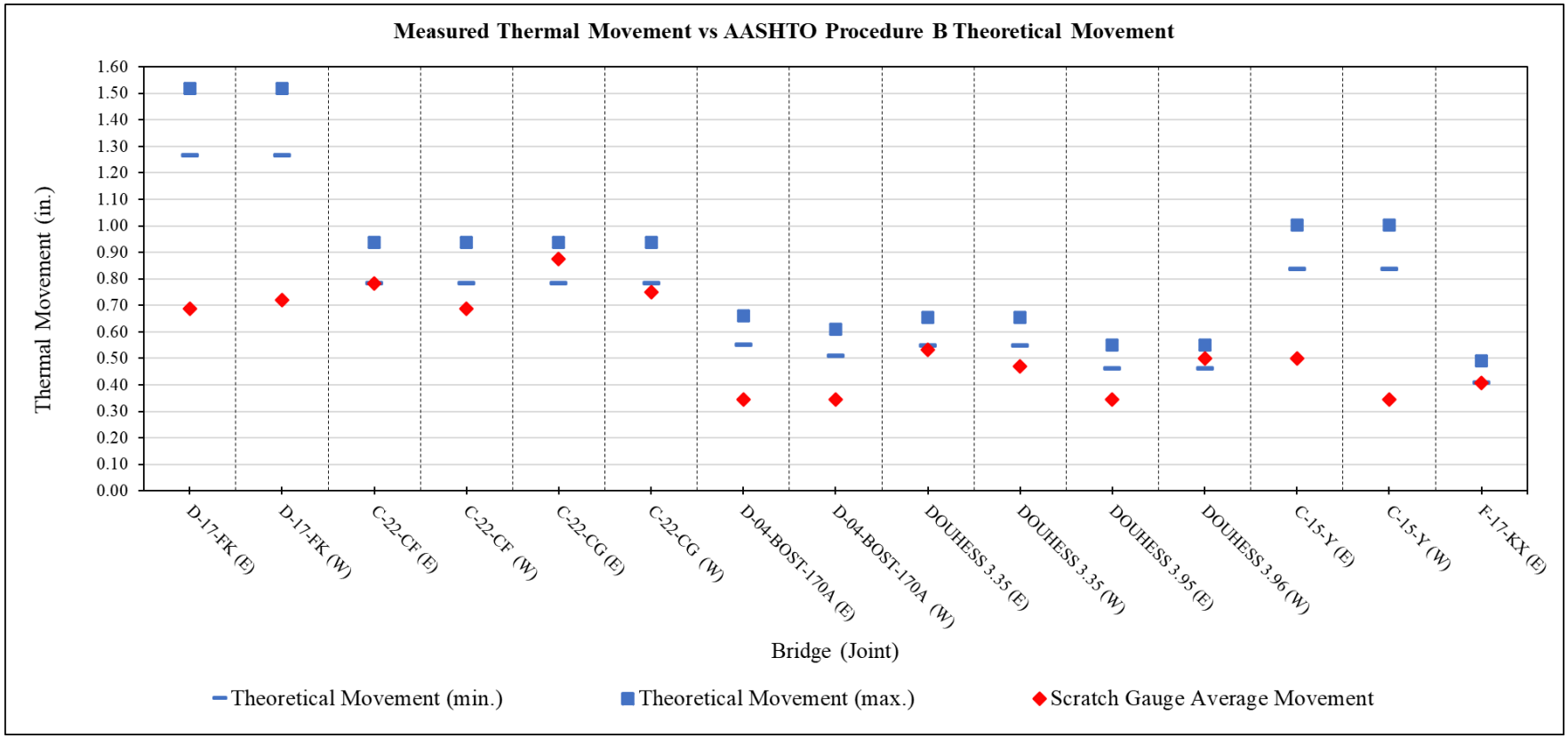

Figure 5-4 Procedure B theoretical movements compared to observed movement

Apart from the two multi-span structures, D-17-FK and C-15-Y, the other six bridges experienced movement within a range of 0.40 inches to 0.06 inches to the theoretical movement calculated per Procedure B.

The accuracy of the predicted joint displacement is compared to the expansion length, *L*, of the bridge in the far right columns of Table 5-4 and Table 5-5. Figure 5-5 plots the difference between the measured and theoretical movement of the bridge joint as a percent of the expansion length versus the expansion length. This figure shows there is no consistent trend relating the prediction error and the expansion length.

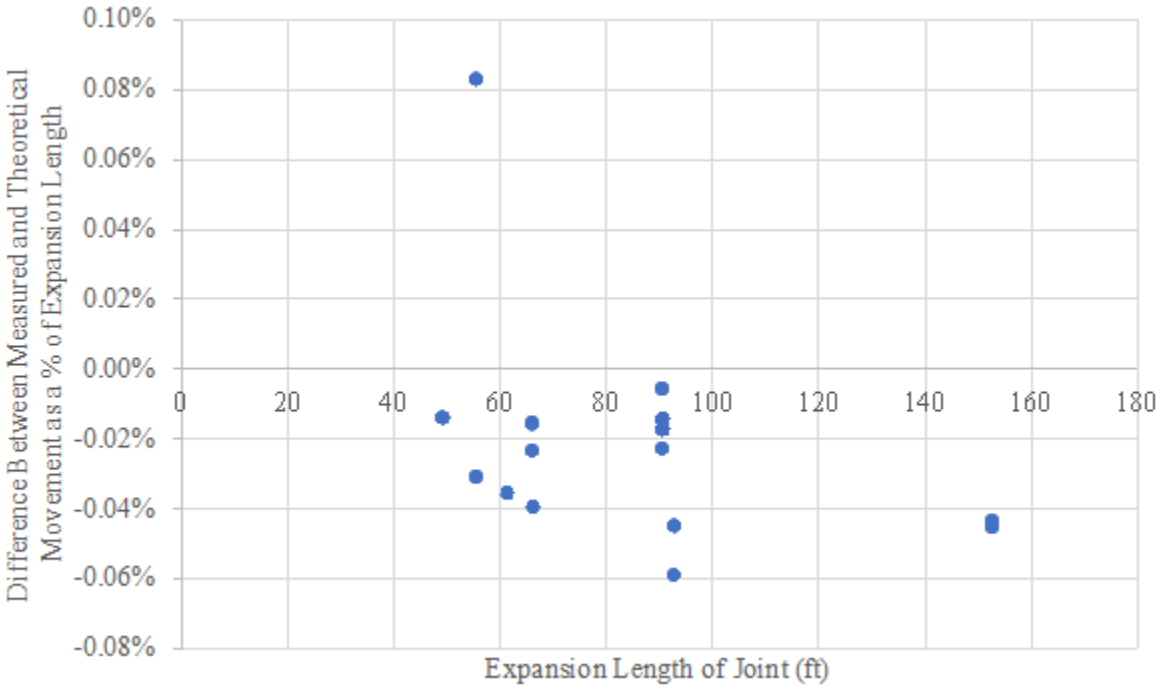

Figure 5-5 Difference Between Measured and Theoretical Joint Movement as a % of Expansion Length Compared to Expansion Length

Effects of Clogged Joints

In theory, bridges which contain joints at zero skew to the structure alignment and allow for unimpeded movement should translate equally across the joint length. Additionally, if the structure is symmetric about the centerline of span and no vertical grade is present, each end of the structure should translate at similar if not identical magnitude. The results presented in Table 5-1 show variable movement both at a single joint and between joints on symmetrical structures, possibly due to uneven joint clogging. As shown in Figure 5-5, variable degrees of joint clogging were observed on all bridges during site and instrumentation visits.

Figure 5-6 Clogged joints observed on multiple bridges within this study

Though undesirable, joint clogging in strip seal joints is virtually unavoidable as sediment, deicing agents, and other foreign bodies are frequently deposited in the opening by passing traffic, weather elements, or snowplows and remain in place until removed by maintenance personnel. Cleaning of joints is a time consuming and costly endeavor considering the number of bridges in any given CDOT Region, thus maintenance does not occur at brief intervals and large sediment build up within the joint can occur. The adverse effects of joint clogging and subsequent effects on thermal bridge movement resulting in structural damage and extensive repairs make small movement joints a desirable option, where applicable, as they provide a reduced opening for larger debris to fill. Further investigation should be done to determine the performance of small movement joints on similar structures.

Discussion

The results presented in this chapter support CDOT's preference for AASHTO Procedure B over AASHTO Procedure A. The results show that the use of Procedure A may result in an undersized joint while Procedure B consistently overestimated thermal bridge movements. Overestimation of the movement a joint will be designed for is preferred to the alternative as an undersized joint will behave similarly to a clogged joint and can result in structural damage. While oversizing a joint is conservative in design and ensures ample openings for thermal movement, the life-time cost associated with installation and maintenance of larger joints may be cause for investigation into the applicability of smaller joints.

Single-span integral bridge joint sizes can be accurately designed per Procedure B while multi-span integral bridge joints were considerably overestimated compared to measurements in this study. The movements of single span box girder and CBT bridges both compared closely to the theoretical values predicted by AASHTO Procedure B. Multi-span structures were considerably overestimated. The largest overestimation of thermal movement for the CBT bridges occurred in bridge D-17-FK, where Procedure B required designing for 0.830 to 0.768 inches more than the movement recorded by the scratch gauges. This may be due to the structure containing two spans with an interior pier where some lateral movement may be dissipated or due to the longer length of the bridge. This is also reflected in box girder bridge C-15-Y which contains an interior pier and an overestimated thermal movement of 0.439 and 0.752 inches

following Procedure B. While bridge D-17-FK is 265.5 feet in length and larger bridge movements and thus variability in movements can be expected, bridge C-15-Y is much shorter at 145.5 feet in length and produces a similar overestimation of bridge movement. Further research into the effects of interior piers for multi-span integral structures in regards to thermal movements should be considered.

The temperature range maps provided in AASHTO Procedure B provide accurate temperature ranges relative to local weather station data for bridges selected in this study. As the effects of global warming and ensuing effects on weather patterns become apparent, updates to said maps should be implemented to accurately reflect temperature ranges. Procedure A uses a much too simplified approach for determining the temperature range due to relying on the annual days below freezing as the climate differentiator between a Moderate or Cold climate. The calculated theoretical movements are then unreliable and underestimate the actual movements the joint will undergo as shown in this study.

Theoretical Reduction Coefficient

Given the results of this study, a reduction coefficient to be used when determining the theoretical thermal movement range is not applicable for single span structures as AASHTO Procedure B closely reflects and overestimates within reason the actual movement observed on instrumented single span bridges. On the contrary, multi-span integral structures tend to translate less than expected using AASHTO Procedure B, as seen with C-15-Y and D-17-FK. With expected thermal movement ranges of 1.002 inches and 1.518 inches, bridges C-15-Y and D-17-FK experienced 0.563 to 0.250 inches and 0.750 to 0.688 inches of joint movement, respectively. Table 5-6 shows the relative difference for each joint on both multi-span structures in an effort to determine a reduction coefficient for future design of similar structures.

Table 5-6 Comparison of joint movement on multi-span bridge to theoretical movement

Bridge	Joint	Corner	Measured (in.)	Theoretical (in.)	Measured/Theoretical
C-15-Y	East	NE	0.563	1.002	56.14%
C-15-Y	East	SE	0.438	1.002	43.66%
C-15-Y	West	NW	0.438	1.002	43.66%
C-15-Y	West	SW	0.250	1.002	24.95%
D-17-FK	East	NE	0.688	1.518	45.29%
D-17-FK	East	SE	0.688	1.518	45.29%
D-17-FK	West	NW	0.750	1.518	49.41%
D-17-FK	West	SW	0.688	1.518	45.29%

Table 5-6 shows that the NE corner of bridge C-15-Y showed the closest correlation to the theoretical value calculated using Procedure B at 56.14%. With all other joint measurements below 50% of the theoretical value, it appears the method described in AASHTO Procedure B is not adequate to accurately predict thermal bridge movements for multi-span integral structures. When calculating the thermal movement range for similar multi-span structures, a reduction coefficient of 0.60 may be applied in AASHTO eq. 3.12.2.3-1 to avoid oversizing the joint. However, this reduction coefficient of 0.60 is based entirely on the maximum correlation of observed to theoretical values in Table 5-6 of 56.14% rounded to the nearest tenth, and this study included only 2 multi-span bridges. Further investigation and testing

should be conducted to validate the use of a reduction coefficient for multi-span integral structures before any changes to design procedures are recommended.

Conclusions

Summary

Bridge expansion joints are required to allow for thermal expansion and contraction but joints can also be a source of costly maintenance issues. Joints can be damaged by snowplows and when the joint is clogged with sediment and foreign objects, the joint may underperform and cause damage to the surrounding components. Departments of Transportation are then faced with the choice of implementing regular joint cleaning, which is both time consuming and costly, or developing an alternative or more accurate joint designs to decrease or eliminate potential adverse consequences from clogged or damaged joints. Although multiple joints studied on this project showed signs of clogging, observed joint movements closely reflected those predicted with AASHTO Procedure B, recommended for use in design per the CDOT BDM.

The results of this study show the necessity for expansion devices on integral bridge structures to allow for thermal movements. The methods for determining the design thermal movement range of a structure contained within AASHTO provide reasonable results for single span CBT and box girder bridges using Procedure B. This procedure is relatively accurate in part due to the accuracy of the temperature maps used to determine the theoretical movement range as well as the design factor of 1.20, used to avoid under -sizing the joint.

Multi-span integral structures were found to not behave as anticipated by Procedure B with a majority of field measurements being less than half the design theoretical thermal movement range. This overestimation of thermal movement can result in costly oversized joints and a maintenance increase throughout the structures' life due to a higher chance of clogging, damage from snowplows, and adverse effects from both. A reduction factor of 0.60, corelating to the 56% maximum thermal movement observed of the total theoretical movement range in bridge C-15-Y, is proposed for initial consideration on multi-span integral structures to still account for thermal movements without overdesigning the expansion joints. This factor would be multiplied by the design thermal movement range found using Procedure B in conjunction with the 1.20 design factor. Further research on multi-span structures should be conducted to validate the use of a reduction factor before being implemented in design.

Limitations

The findings of this study should be considered in light of several limitations. In this study joint displacements of six CBT girder and two concrete box girder bridges were monitored for slightly longer than one year. Effort was made to select representative bridges, but further study considering more bridges, more variable climate conditions, and longer exposure times would give additional confidence in the finding that the AASHTO Procedure B procedures are appropriate for single span structures. The scratch gauges have been left in place to allow for future monitoring, and the scratch gauges are fairly inexpensive to manufacture and install. Additional gauges could be installed at bridges around the state and joint movements could be routinely monitored by maintenance personnel to collect a more extensive database of joint movement.

Multi-span CBT girder and concrete box girder bridges with integral abutments deserve focused study. Only two multi-span bridges were included in the study bridges and both of these bridges showed much smaller joint movements than expected. There is the potential that these bridge joints could be designed differently with additional information, but given the damage to abutments and other bridge elements that can result when expansion is not accommodated, study of many additional bridges is needed before a design change can be safely made.

References

American Chemistry Council. (2022, October 14). Neoprene. ChemicalSafetyFacts.org https://www.chemicalsafetyfacts.org/chemicals/neoprene/#:~:text=Neoprene%20is%20a%20synthetic%20rubber,solvents%20and%20water%20through%20vulcanization.

American Association of State Highway and Transportation Officials. (2020). AASHTO LRFD Bridge Design Specifications 9th Edition.

Arsoy, S., Barker, R.M., and Duncan, J.M. (1999). The Behavior of Integral Abutment Bridges. Virginia Transportation Research Council. https://www.virginiadot.org/vtrc/main/online_reports/pdf/00-cr3.pdf

Caltrans Division of Research, Innovation and System Information. (2019). Maintenance Practices for Bridge Drains and Expansion Joints: Survey of Practice. https://dot.ca.gov/-/media/dot-media/programs/research-innovation-system-information/documents/preliminary-investigations/maintenance-practices-for-bridge-drains-and-expansion-joints-survey-of-practice-pi-a11y.pdf

Burgdorfer, R., Berman,G.W. and Roeder, C.W. (2013). Standard Practice for Washing and Cleaning Concrete Bridge Decks and Substructure Bridge Seats Including Bridge Bearings and Expansion Joints to Prevent Structural Deterioration. Washington State Transportation Center. https://depts.washington.edu/trac/bulkdisk/pdf/811.2.pdf

Chang, L. M., & Lee, Y. J. (2002). Evaluation of performance of bridge deck expansion joints. Journal of performance of constructed facilities, *16*(1), 3-9.

Colorado Department of Transportation. (2023). Bridge Design Manual. https://www.codot.gov/programs/bridge/bridge-manuals/design_manual?b_start:int=0

Davidson, E., White, D., and Khan, L. (2012). Evaluation of Performance and Maximum Length of Continuous Decks in Bridges – Part 2. Georgia Institute of Technology, School of Civil and Environmental Engineering, Structural Engineering, Mechanics, and Materials Research Report. https://www.gti.gatech.edu/sites/default/files/u51/RP%2010-29_Final%20Report.pdf

Environmental Protection Agency. (2023, November 20). *Heat Island Effect.* https://www.epa.gov/heatislands#:~:text=Urban%20areas%2C%20where%20these%20structures,2%2D5%C2%B0F%20higher.

Federal Highway Administration. (2016). Portland Cement Concrete Pavements Research: Thermal Coefficient of Portland Cement Concrete. https://www.fhwa.dot.gov/publications/research/infrastructure/pavements/pccp/thermal.cfm

Frosch, R. J., & Lovell, M. D. (2011). Long-term Behavior of Integral Abutment Bridges. Publication FHWA/IN/JTRP- 2011/16. Joint Transportation Research Program, Indiana Department of Transportation and Purdue University, West Lafayette, Indiana. DOI: 10.5703/1288284314640

Li, L., Chen, B., Zhou, L., Xia, Q., Zhou, Y., Zhou, X., & Xia, Y. (2023). Thermal behaviors of bridges—A literature review. Advances in Structural Engineering, *26*(6), 985-1010.

Liu, H., Han, J., & Parsons, R. L. (2022). Integral bridge abutments in response to seasonal temperature changes: State of knowledge and recent advances. Frontiers in Built Environment, *8*, 916782.

LaFave, J.M., Fahnestock, L.A., Brambila, G., Riddle, J.K., Jarrett, M.W., Svatora, J.S., Wright, B.A., and An, H. (2017). Integral Abutment Bridges under Thermal Loading: Field Monitoring and Analysis. Illinois Center for Transportation. https://doi.org/10.36501/0197-9191/17-022

National Weather Service. (n.d) NOWData – NOAA Online Weather Data. https://www.weather.gov/wrh/climate

Phares, B. M., Faris, A. S., Greimann, L., & Bierwagen, D. (2013). Integral bridge abutment to approach slab connection. Journal of Bridge Engineering, 18(2), 179-181.

Bridge Schematics

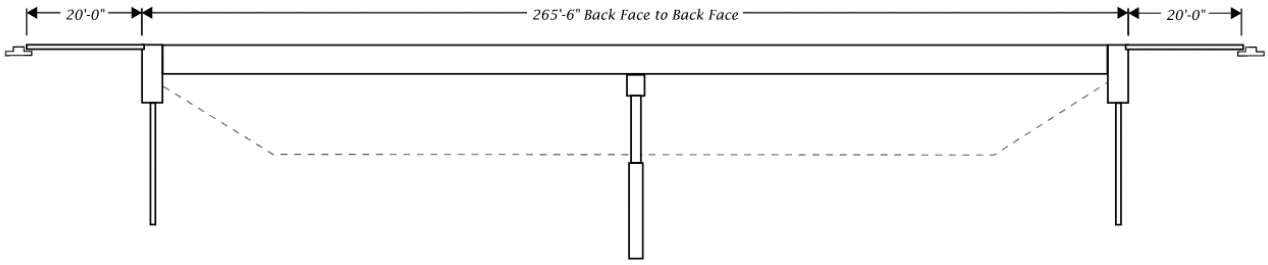

Figure A-1 Bridge D-17-FK schematic

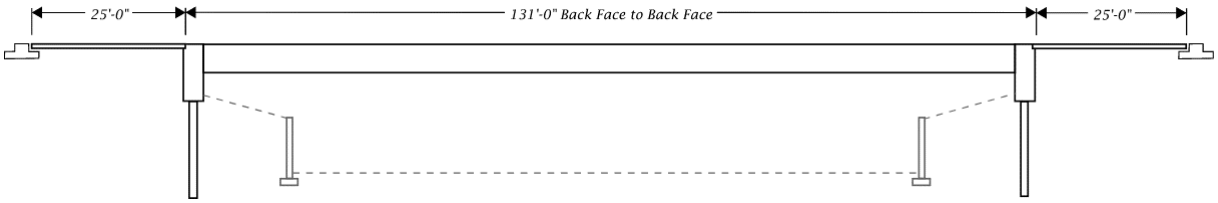

Figure A-2 Bridges C-22-CF and C-22-CG schematics

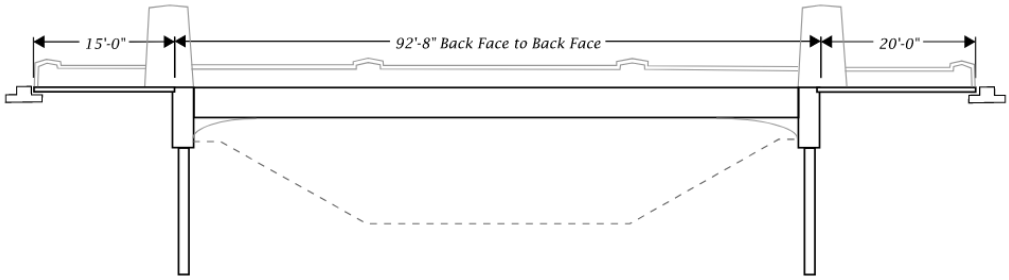

Figure A-3 Bridge D-04-BOST-170A schematic

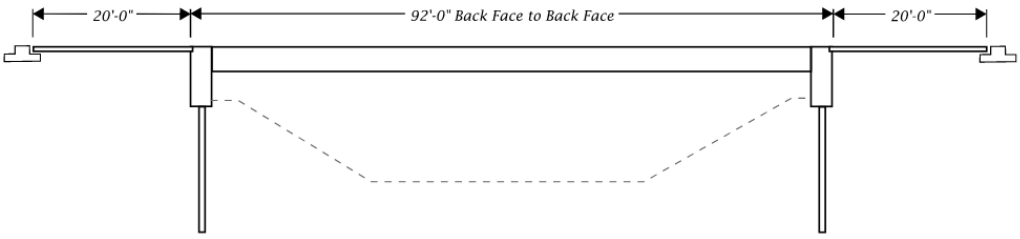

Figure A-4 Bridge DOUHESS-3.35 schematic

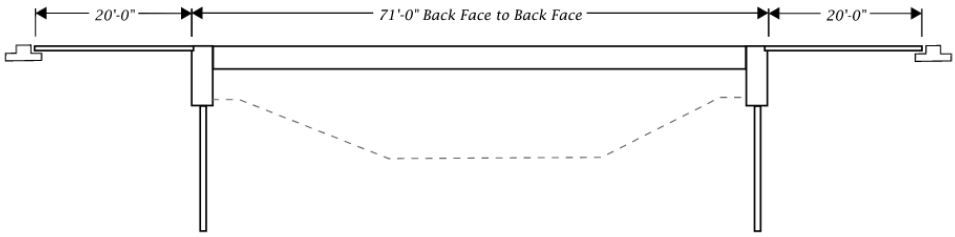

Figure A-5 Bridge DOUHESS-3.95 schematic

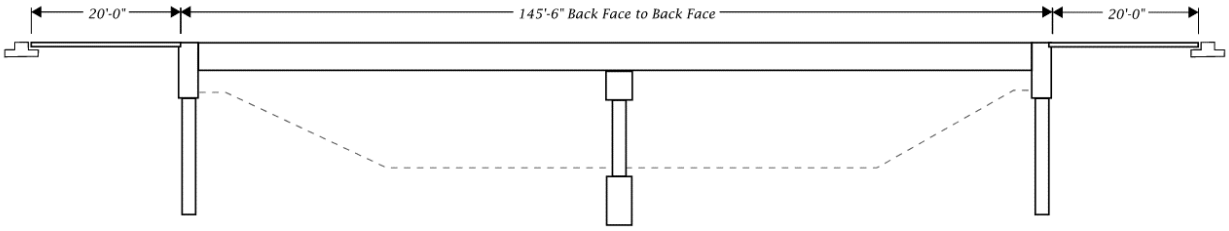

Figure A-6 Bridge C-15-Y schematic

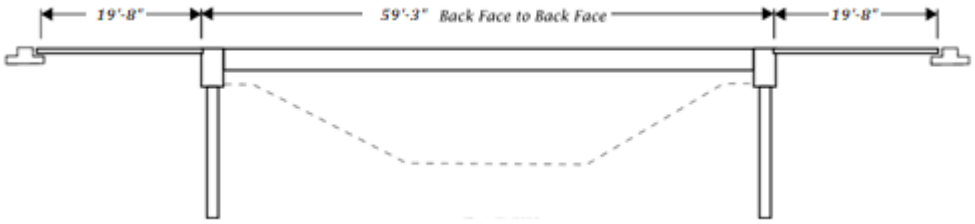

Figure A-7 Bridge F-17-KX schematic

Scratch Gauge Design/Construction

The scratch gauges are made out of 1/16” thick aluminum plate. The scratch gauge is 9.5” long by 2” wide. The aluminum is first scuffed with 80 grit sandpaper to allow the primer and paint to adhere better (Figure B-1). The aluminum is then coated with two coats of Rust-oleum red sandable primer. This is then coated with two coats of Rust-oleum black high performance enamel. The red primer followed by a black topcoat was selected in the belief that even light scratches would be easy to see and measure.

The stylus is a screw that has been filed down to a point. It is held in place by two nuts. The nuts are kept in place and not allowed to come loose using blue Loctite. The stylus arm is 1” wide and is 1/8” mild steel. 1/8” thickness was selected to keep the flex of the stylus arm to a minimum.

Figure B-1 A scratch gauge that has been scuffed by sandpaper

Figure B-2 A scratch gauge that has been spray painted with a black enamel coating